

Impact of Enhanced Malaria Control on the Competition between *Plasmodium falciparum* and *Plasmodium vivax* in India

Olivia Prosper^{1*}, Maia Martcheva¹

¹Department of Mathematics, University of Florida,
358 Little Hall, PO Box 118105,
Gainesville, FL 32611-8105

September 12, 2011

Abstract

The primary focus of malaria research and control has been on *P. falciparum*, the most severe of the four *Plasmodium* species causing human disease. However, the presence of both *Plasmodium falciparum* and *Plasmodium vivax* occurs in several countries, including India. We developed a mathematical model describing the dynamics of *P. vivax* and *P. falciparum* in the human and mosquito populations and fit this model to Indian clinical case data to understand how enhanced control measures affect the competition between the two *Plasmodium* species. Around 1997, funding for malaria control in India increased dramatically. Our model predicts that if India had not improved its control strategy, the two species of *Plasmodium* would continue to coexist. To determine which control measures contributed the most to the decline in the number of cases after 1997, we compared the fit of seven models to the 1997-2010 clinical case data. From this, we determined that increased use of bednets contributed the most to case reduction. During the enhanced control period, the best model predicts that *P. vivax* is out-competing *P. falciparum*. However, the reproduction numbers are extremely close to the invasion boundaries. Consequently, we cannot be confident that this outcome is the true future of malaria in India. We address this uncertainty by performing a parametric bootstrapping procedure for each of the seven models. This procedure, applied to the enhanced control period, revealed that the best model predicts that *P. vivax* outcompeting *P. falciparum* is the most likely outcome, whereas the remaining candidate models predict the opposite. Moreover, the predictions of the top model are counter to what one expects based on the case data alone. Although the proportion of cases due to *falciparum* has been increasing, the best fitting model reveals that this observation is insufficient to draw conclusions about the longterm competitive outcome of the two species.

*Corresponding author, e-mail: oprosper@ufl.edu

1 Introduction

Roughly 250 million people suffer from malaria infection each year, resulting in nearly one million deaths [32]. Malaria is the fifth leading killer among infectious diseases worldwide, and it is the second leading cause of death in Africa, behind HIV/AIDS [6]. Despite many attempts at controlling malaria in India over the past sixty years, India still produces roughly 70% of the malaria cases within Southeast Asia, resulting in about two million cases and 1000 deaths each year. While mortality due to *Plasmodium* infection is low in India relative to the total morbidity, malaria still poses an enormous burden to the country. Several factors, including the biology and epidemiology of the disease, emerging drug-resistance of parasites, insecticide resistance of mosquitoes, and socio-economic barriers, have proven to be difficult obstacles to overcome in the ongoing pursuit of malaria control.

1.1 *Plasmodium vivax* and *Plasmodium falciparum* parasites and obstacles they pose to malaria control

P. vivax and *P. falciparum* have very similar life cycles, with one important exception. When a human is infected by a mosquito with *P. vivax*, some of the parasites become hypnozoites, which can remain dormant in the human liver cells for some time, then reactivate. Consequently, individuals infected with *P. vivax* are prone to relapses. In fact, *P. vivax* infections exhibit relapses roughly 30% of the time after the initial clinical episode [1]. Fortunately, *P. falciparum* parasites do not have a hypnozoite stage, and thus relapses do not occur in *falciparum* infections.

Despite the absence of relapse in *falciparum* malaria infections, *P. falciparum* is associated with the highest risk of mortality for humans among the malaria parasite species. *Vivax* infections are considered to be benign, however the symptoms are still debilitating and diminish both a person's quality of life and their productivity. Moreover, some recent cases of *P. vivax* malaria have been far more severe than is traditionally expected of this disease, sometimes resulting in death. The liver stages of *P. vivax* can also be extremely long, up to three years, allowing *P. vivax* parasites to lay dormant and weather the low transmission seasons until conditions have improved, making *vivax* in some respects, a more formidable foe than *P. falciparum* in terms of malaria control.

Although symptoms due to malaria infection can be quite severe and sometimes deadly, it is likely that, because multiple infections can temporarily build a person's immunity to the disease, a large proportion of malaria cases in India are asymptomatic or display very mild symptoms, particularly in regions with meso- to hyper-endemicity [17]. A study of malaria infection in pregnant women in Jharkhand State, India, found that nearly half of the women in the study carried asymptomatic malaria infection [15]. Since asymptomatic human malaria infections are still infectious to mosquitoes, unlikely to be treated, and consequently longer-lived, asymptomatic humans, in addition to liver stage *vivax* infected humans, create a reservoir for malaria parasites. Furthermore, the long duration of untreated or unsuccessfully treated infections increases the likelihood

of co-infection with *P. vivax* and *P. falciparum* species. It can be very difficult to identify malaria co-infections because it is not yet very well understood how the two species interact. Co-infected individuals can also be very difficult to treat because a drug that works for one infection may confer resistance in the other.

1.2 Objectives of modeling *P. vivax*-*P. falciparum* disease dynamics

In this paper, we develop a *P. vivax*-*P. falciparum* malaria model with co-infection to address questions regarding control measures in the context of India. We want to find out what effect certain control measures have on the competition between the two parasite species, how the presence of two circulating parasites affects what control measures should be implemented and how they can best be implemented. The current literature on malaria in India dictates that there is a need to address not only *Plasmodium falciparum* malaria, which is more commonly studied and modeled, but *Plasmodium vivax* as well. Chiyaka et al. have published the first two-species malaria model, incorporating *P. falciparum* and *P. malariae* [7]. However, there is still a need to model *P. falciparum* and *P. vivax* disease dynamics, particularly because the epidemiology of these two parasites is so different. These differences, which are intrinsic to the parasite biology and are likely to greatly enhance the parasites' ability to persist in a population in the face of numerous control efforts, need to be included in a mathematical model if we want to provide insight into problems regarding competition between parasite species in India and how to develop an effective control policy for India. In Section 2, we introduce the two-parasite ordinary differential equation malaria model. In Section 2.5 we present the disease-free equilibrium, the basic reproductive number for the model, and the control reproductive number. We present the isolated endemic equilibria of the system in section 2.7 and a complete description and interpretation of the invasion numbers in Section 2.8. Section 3 explains the parameters used in the model and the values chosen for each parameter. In Section 3.3, for the 1987-1996 period, we estimate transmission parameters by fitting the ODE model to Indian malaria case data. Comparison of several models for the enhanced control period (1997-2010) in Section 3.4 allowed us to determine which control measures contributed the most to the success of control programs. In the same section, we also present an uncertainty analysis to determine the most likely outcome of malaria in India.

2 *P. falciparum* and *P. vivax* Malaria Co-infection Model

In the two-parasite malaria model below, it is assumed that the mosquito population size, N_m , is constant, and that the size of the human population, N , exhibits logistic growth. The state variable M denotes the number of mosquitoes that are fully susceptible to both *P. vivax* and *P. falciparum* parasites. Similarly, S denotes the number of humans who are fully susceptible to both malaria parasites. The number of infected mosquitoes at a given time is J , the sum of *P. vivax* infected mosquitoes (J_v) and *P. falciparum* infected mosquitoes (J_f).

Human deaths due to *P. vivax* infection are rare, and are thus considered to be negligible. Although deaths due to *P. falciparum* do occur, the associated mortality rate in India is very small compared with the total morbidity due to malaria. Once infectious individuals recover fully from malaria, they again become susceptible to malaria infection and move to class S . As a result, in this two-parasite model, all humans recover from malaria infection. Once infectious individuals recover fully from malaria, they again become susceptible to malaria infection and move to class S . Thus, when we refer to an individual “surviving” a particular stage, we mean that they did not die due to natural mortality before the end of that stage.

2.1 Modeling the dynamics of *Plasmodium vivax* infection in the human population

First, we describe the dynamics of *P. vivax* malaria in the human population. When a *P. vivax* infected mosquito successfully transmits a malaria parasite to a human, we assume that these humans first go through a liver stage, denoted by L , in which the malaria parasites remain un-infectious. This liver stage acts as both the initial incubation period for the *P. vivax* malaria parasites in a human and as the period between relapses in which malaria parasites remain in a dormant liver stage as hypnozoites. Because asymptomatic individuals create a reservoir for malaria, posing significant challenges to malaria control, and because malaria infected individuals do not become infectious until the parasites have gone through the human liver stage [2], the model allows for a fraction of the individuals in the liver stage to bi-pass the symptomatic stage and move directly to the *P. vivax* infectious stage I_v . We refer to individuals who bi-pass the symptomatic stage as “asymptomatic”, and those who do not are referred to as “symptomatic”.

A human presenting symptoms is considered a “clinical case” and we let C_v denote the *P. vivax* clinical cases at any given time. Assuming an individual in C_v does not die of natural mortality, he or she will become infectious and move into the I_v stage. Once in this infectious stage, individuals have the potential to fully recover, returning to the susceptible class S via either successful treatment or natural recovery. We assume that although individuals may begin treatment during the clinical stage, the treatment does not affect the person’s progression to the infectious stage. Consequently, we assume that even in treated individuals, gametocyte clearance (loss of infectiousness) occurs in the infectious stage.

As described previously, because some *P. vivax* parasites become hypnozoites during the liver stage, remain dormant in the liver for some period, and are reactivated at a later time, *vivax* malaria patients who are not successfully treated are prone to relapses. Thus, in our model, individuals in the *vivax* infectious class I_v can return to the liver stage L and repeat the cycle of the *vivax* infection.

2.2 Modeling the dynamics of *Plasmodium falciparum* infection in the human population

Plasmodium falciparum infections, while typically more severe than *vivax* infections, exhibit simpler infection dynamics than *vivax* infections. In particular, *P. falciparum* parasites do not have a hypnozoite stage, and consequently, individuals infected with only *P. falciparum* do not experience relapses. In light of this difference between *P. falciparum* and *P. vivax* infections, we omit the *falciparum* incubation period which is typically shorter than that of *P. vivax*, meaning that once a human is infected by a *P. falciparum* infectious mosquito, that individual moves directly either to the *falciparum* clinical stage C_f , or moves to the *falciparum* infectious stage I_f . As noted in the description of *vivax* infection dynamics, we refer to the individuals who bi-pass the clinical stage as “asymptomatic” individuals. Those who pass through the clinical stage are referred to as “symptomatic” individuals. Once in the *P. falciparum* infectious stage, as with *P. vivax* infection, individuals can fully recover via either successful treatment or natural recovery.

The state variables I_v and I_f include both asymptomatic infectious individuals and infectious individuals who have shown symptoms. It will be assumed that symptomatic individuals are treated and asymptomatic individuals are not treated. Thus, the recovery rate from I_v and I_f will be a function of both the natural recovery rate and the treatment-recovery rate.

2.3 Modeling co-infection

Gupta et al. used 180 samples from six endemic regions in India to estimate the proportion of malaria cases that are mixed infections. The samples showed that roughly 46% of the malaria infections were *P. falciparum*–*P. vivax* co-infections [14]. Consequently, the ability for humans to obtain concurrent malaria infections should play an important role in a *P. falciparum*–*P. vivax* malaria model for India. Mixed infection is incorporated into the model by introducing two more “clinical case” state variables, C_{vf} and C_{fv} . A *P. vivax* infected individual in either the liver stage or the infectious stage who becomes co-infected with *falciparum* will move to C_{vf} . At this stage we assume that individuals coming from the liver stage become infectious with *vivax*, those arriving from the infectious stage remain infectious with *vivax*, and all individuals in C_{vf} show symptoms of malaria infection, although it may not be clear which infection is causing the symptoms. According to Snounou et al., the assumption that co-infection with *P. falciparum* can reactivate hypnozoites in the dormant liver-stage, producing *P. vivax* blood-stage parasites, is plausible [30]. Similarly, a *P. falciparum* infectious individual can become co-infected with *P. vivax*. These individuals will move to the C_{fv} stage provided they have not succumbed to natural mortality. Individuals in C_{fv} are still infectious with *P. falciparum*, but present symptoms associated with *P. vivax* infection. We will refer to individuals who have been in stages C_{vf} and C_{fv} as “*vivax* co-infected” and “*falciparum* co-infected” individuals, respectively. If a co-infected individual survives the clinical stage, they become infectious with both malaria parasites and move to I_c .

In this two-parasite model, we assume that all co-infected individuals are treated during the infectious co-infected stage I_c . This assumption is reasonable since most co-infected individuals show symptoms [30]. The question is, what treatment do we give these co-infected individuals? According to the 2009 malaria diagnosis and treatment guidelines for India, *P. falciparum*–*P. vivax* co-infected individuals should be given the same treatment that is given to *P. falciparum* infected patients [23]. However, malaria diagnostic tests often only detect one of the two parasite species in the host, leading health-care providers to treat only the observed infection [20]. When only one of the two infections is treated, symptoms for the other malaria infection emerge anywhere from 17 to 63 days post-treatment [21]. The model incorporates this emergence of the hidden infection by allowing individuals in the infectious co-infected class I_c to move into either I_v or I_f after recovery from the initial observed (and hence treated) infection. If *P. falciparum* is treated first, then the *P. vivax* infection will emerge and individuals move into the infectious class I_v . Likewise, those who are treated for *P. vivax* first move to the infectious class I_f some time post-*vivax* treatment. In our model, however, individuals treated for *P. vivax* first will not show symptoms following treatment of the co-infection since *falciparum* symptoms do not occur following *falciparum* infectiousness. Only co-infected individuals treated for *P. falciparum* first have the possibility of developing symptoms, in particular *vivax* symptoms, since individuals in I_v can relapse. Consequently, our model does not capture the phenomenon described above where *P. falciparum* symptoms emerge following *vivax* treatment. This discrepancy can be resolved by adding a *P. falciparum* incubation period to the model, however for simplicity, and because the majority of co-infections are treated for *P. falciparum* first, followed by the onset of *P. vivax* symptoms, we find that incorporating only a *vivax* incubation/liver stage sufficient to capture the most important features of the two-parasite species disease dynamics.

2.4 Disease dynamics in the mosquito population

The human component of the two-parasite malaria model includes five infectious classes: two classes are infectious with *vivax* only (I_v and C_{vf}), two classes are infectious with *falciparum* only (I_f and C_{fv}), and one class is infectious with both *vivax* and *falciparum* (I_c). Thus, mosquitoes have five means by which they can become infected. A susceptible mosquito infected by a human in class I_v or C_{vf} will develop a *P. vivax* infection. A susceptible mosquito infected by a human in class I_f or C_{fv} will develop a *P. falciparum* infection. In the event that a mosquito becomes infected by a co-infected infectious human (I_c), the model assumes that the mosquito will contract only one of the two malaria parasite species. Which species it contracts will depend on the probability of “picking up” that particular species. Since mosquitoes have a short lifespan, we assume that all mosquitoes die natural deaths rather than disease-induced deaths. A summary of all state variables is given in Table 1. A description of the model parameters, as well as the estimates used in later model simulations, is given in Tables 2 and 3.

The two-parasite malaria model diagram in Figure 1 can be described mathematically as follows:

Table 1: Description of model State Variables at time t .

State Variables	Description
N_m	Mosquito population size - defined to be constant
$N(t)$	Human population size at time t
$M(t)$	Number of susceptible mosquitoes at time t
$S(t)$	Number of susceptible humans at time t
$m(t)$	Proportion of mosquitoes that are susceptible at time t
$J_v(t)$	Number of <i>P. vivax</i> infected mosquitoes at time t
$J_f(t)$	Number of <i>P. falciparum</i> infected mosquitoes at time t
$j_v(t)$	Proportion of mosquitoes that are <i>P. vivax</i> infected at time t
$j_f(t)$	Proportion of mosquitoes that are <i>P. falciparum</i> infected at time t
$L(t)$	Number of human <i>P. vivax</i> liver stage infections at time t
$C_v(t)$	Number of human <i>P. vivax</i> cases at time t
$C_f(t)$	Number of human <i>P. falciparum</i> cases at time t
$I_v(t)$	Number of <i>P. vivax</i> infectious humans at time t
$I_f(t)$	Number of <i>P. falciparum</i> infectious humans at time t
$C_{vf}(t)$	Number of symptomatic co-infected cases, infectious with <i>P. vivax</i> only, at time t
$C_{fv}(t)$	Number of symptomatic co-infected cases, infectious with <i>P. falciparum</i> only, at time t
$I_c(t)$	Number of co-infected humans infectious with both <i>P. vivax</i> and <i>P. falciparum</i> at time t

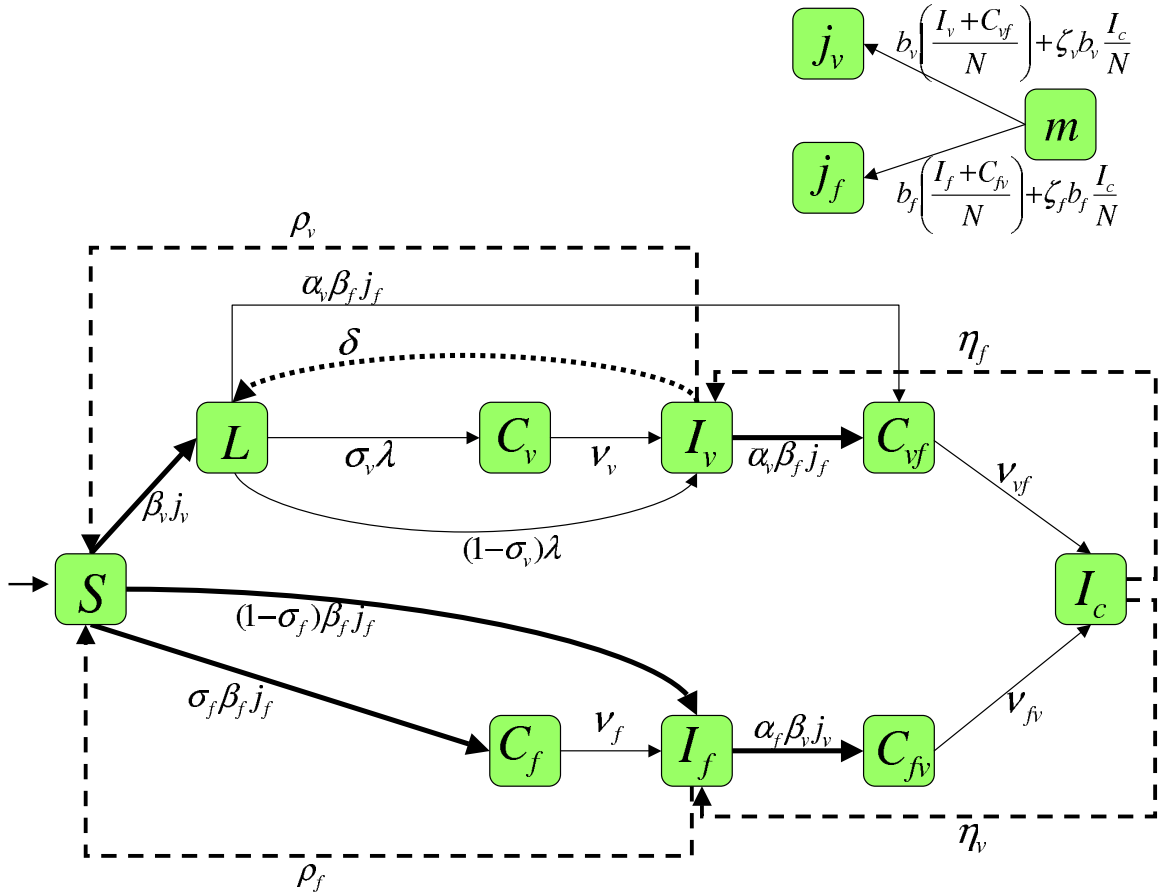


Figure 1: Mosquito and Human Population Dynamics Diagram under the influence of two circulating malaria parasites. Bold arrows indicate the acquisition of a new infection, and dotted arrows indicate recovery from either *P. vivax* or *P. falciparum* infection.

Mosquito Dynamics:

$$\frac{dJ_v}{dt} = b_v \left(\frac{I_v + C_{vf}}{N} \right) (N_m - J) + \zeta b_v \frac{I_c}{N} (N_m - J) - dJ_v \quad (1)$$

$$\frac{dJ_f}{dt} = b_f \left(\frac{I_f + C_{fv}}{N} \right) (N_m - J) + (1 - \zeta) b_f \frac{I_c}{N} (N_m - J) - dJ_f \quad (2)$$

where $J \doteq J_v + J_f$, N_m is constant, and $M = N_m - J$.

Since it is difficult to estimate how large the mosquito population is, we modify the mosquito dynamics equations by considering the proportion of mosquitoes infected rather than the number of mosquitoes infected. Thus, dividing equations (1) and (2) by the total mosquito population size N_m , we arrive at the following set of equations describing the mosquito infection dynamics:

$$\begin{aligned} \frac{dj_v}{dt} &= b_v \left(\frac{I_v + C_{vf}}{N} \right) (1 - j) + \zeta b_v \frac{I_c}{N} (1 - j) - dj_v \\ \frac{dj_f}{dt} &= b_f \left(\frac{I_f + C_{fv}}{N} \right) (1 - j) + (1 - \zeta) b_f \frac{I_c}{N} (1 - j) - dj_f \end{aligned}$$

where now $j \doteq j_v + j_f = \frac{1}{N_m}(J_v + J_f)$, denotes the fraction of the mosquito population that is infected with malaria parasites and hence, $m = 1 - j$ represents the fraction of mosquitoes that are susceptible to malaria infection. Note that

$$m' = -j' = - \left(b_v \left(\frac{I_v + C_{vf}}{N} \right) + \zeta b_v \frac{I_c}{N} + b_f \left(\frac{I_f + C_{fv}}{N} \right) + (1 - \zeta) b_f \frac{I_c}{N} \right) m - d(1 - m).$$

In the above system, b_v and b_f are human-to-mosquito transmission rates, d is the mosquito natural mortality rate, and ζ is the probability that if a susceptible mosquito bites an I_c human, the mosquito will contract *vivax* rather than *falciparum*.

Human Dynamics:

$$\begin{aligned}
\frac{dS}{dt} &= \frac{dN}{dt} - \frac{dL_v}{dt} - \frac{dC}{dt} - \frac{dI}{dt} \\
&= rN \left(1 - \frac{N}{K}\right) + \rho_v I_v + \rho_f I_f - (\beta_v j_v + \beta_f j_f) S - \mu S \\
\frac{dL}{dt} &= \beta_v S j_v + \delta I_v - \alpha_v \beta_f j_f L - (\lambda + \mu) L \\
\frac{dC_v}{dt} &= \sigma_v \lambda L - (\nu_v + \mu) C_v \\
\frac{dI_v}{dt} &= (1 - \sigma_v) \lambda L + \nu_v C_v + \eta_f I_c - \alpha_v \beta_f I_v j_f - (\delta + \rho_v + \mu) I_v \\
\frac{dC_{vf}}{dt} &= \alpha_v \beta_f (I_v + L) j_f - (\nu_{vf} + \mu) C_{vf} \\
\frac{dC_f}{dt} &= \sigma_f \beta_f S j_f - (\nu_f + \mu) C_f \\
\frac{dI_f}{dt} &= (1 - \sigma_f) \beta_f S j_f + \nu_f C_f + \eta_v I_c - \alpha_f \beta_v I_f j_v - (\rho_f + \mu) I_f \\
\frac{dC_{fv}}{dt} &= \alpha_f \beta_v I_f j_v - (\nu_{fv} + \mu) C_{fv} \\
\frac{dI_c}{dt} &= \nu_{vf} C_{vf} + \nu_{fv} C_{fv} - (\eta_v + \eta_f + \mu) I_c
\end{aligned}$$

where $C \doteq C_v + C_f + C_{vf} + C_{fv}$, $I \doteq I_v + I_f + I_c$, and the total population size is described by the logistic equation $\frac{dN}{dt} = rN \left(1 - \frac{N}{K}\right) - \mu N$.

The mosquito-to-human transmission rates for *vivax* and *falciparum* are denoted by β_v and β_f , respectively. The natural human mortality rate is given by μ . A proportion σ_v of *vivax* and a proportion σ_f of *falciparum* cases are symptomatic. We assume symptomatic individuals get treated and clear blood-stage parasites at a rate γ_i from infection i and asymptomatic individuals clear blood-stage parasites at a rate r_i ($i = v, f$). Thus, the rates of returning to the susceptible class, denoted by ρ_v and ρ_f , are a function of both treatment and natural parasite-clearance rates: $\rho_i = \sigma_i \gamma_i + (1 - \sigma_i) r_i$, for $i = v, f$. *Vivax*-infected individuals progress at a rate λ from the liver stage to either C_v or I_v . *Vivax*-symptomatic and *falciparum*-symptomatic individuals progress to the infectious stage at rate ν_v and ν_f , respectively. Similarly, *vivax*-co-infected and *falciparum*-co-infected individuals enter I_c at rates ν_{vf} and ν_{fv} , respectively. α_v and α_f are cross-immunity coefficients. δ is the rate at which *vivax*-infected individuals relapse. This parameter is given by $\delta = p_r \sigma_v \gamma_f + (1 - \sigma_v) r_v$, where p_r is the probability that a treated *vivax* patient relapses. Finally, η_v and η_f are the probabilities that an I_c individual is treated first for *vivax* and, respectively, for *falciparum* infection. A complete list of the model parameters and their descriptions is presented in Tables 2 and 3.

2.5 Derivation of the disease-free equilibrium, basic reproductive number R_0 and control reproductive number R_C

Note that $\frac{dN}{dt}$ can be rewritten in the form $\frac{dN}{dt} = (r - \mu)N \left(1 - \frac{N}{K(1 - \frac{\mu}{r})}\right)$ so that the intrinsic growth rate of the population \hat{r} is $r - \mu$, and the carrying capacity \hat{K} is $K \left(1 - \frac{\mu}{r}\right)$.

The disease-free equilibrium is $(N^*, m^*, j_v^*, j_f^*, S^*, L^*, C_v^*, C_f^*, I_v^*, I_f^*, C_{vf}^*, C_{fv}^*, I_c^*)_{DFE} = (\hat{K}, 1, 0, 0, \hat{K}, 0, 0, 0, 0, 0, 0, 0, 0)$. N^* and S^* are easily determined by setting the right hand side of $\frac{dN}{dt} = \hat{r}N \left(1 - \frac{N}{\hat{K}}\right)$ equal to zero and noting that when there is no disease, $S = N$. Since $m^* = 1 - j^*$, we have that $m^* = 1$ when there is no disease.

The basic reproductive number, R_0 , of an epidemiological model is the average number of secondary cases produced by one infectious individual in an otherwise fully susceptible population where no control is being implemented. The control reproductive number, R_C , is defined similarly, with the exception that control measures are assumed to be in place. If $R_0 < 1$, the disease-free equilibrium is locally asymptotically stable, implying that the disease will eventually become extinct. On the other hand, if $R_0 > 1$, the disease-free equilibrium is unstable [31]. Consequently, determining an expression for the basic reproductive number from the model and estimating its value is a key component to understanding how difficult it will be to control transmission of the disease and what control measures will be the most effective. An important goal of any infectious disease control program is to implement control measures in such a way as to successfully bring the control reproductive number below one. The isolation reproductive numbers of a multi-parasite model, such as this two-parasite malaria model, are the basic reproductive numbers for the model when only one parasite species is present at a time.

2.6 Expression of R_C and R_0 derived from the next generation approach

Using the next generation operator approach [31], we find that the control reproductive number (R_C) for the malaria model is given by $R_C = \max\{R_{Cv}, R_{Cf}\}$, where R_{Cv} is the isolation control reproductive number for *P. vivax*, and R_{Cf} is the isolation control reproductive number for *P. falciparum*. For details of the derivation of R_C , see appendix A.1. These isolation control reproductive number for *P. falciparum* is described by the expression below:

$$R_{Cf} = \sqrt{\frac{\beta_f}{d} \cdot \left[(1 - \sigma_f) + \sigma_f \frac{\nu_f}{\nu_f + \mu} \right] \frac{b_f}{\rho_f + \mu}} \quad (3)$$

$$= \sqrt{R_{Cf}^a + R_{Cf}^s}, \quad (4)$$

where

$$R_{Cf}^a = \frac{\beta_f}{d} \cdot (1 - \sigma_f) \cdot \frac{b_f}{\rho_f + \mu} \quad (5)$$

$$R_{Cf}^s = \frac{\beta_f}{d} \cdot \sigma_f \cdot \frac{\nu_f}{\nu_f + \mu} \frac{b_f}{\rho_f + \mu}. \quad (6)$$

Observe that R_{Cf}^a is the contribution of an asymptomatic infectious individual to the basic reproductive number and R_{Cf}^s is the contribution of a symptomatic infectious individual.

The *P. vivax* isolation control reproductive number is given by

$$R_{Cv} = \sqrt{\frac{R_{Cv}^a + R_{Cv}^s}{1 - \frac{\delta}{\delta + \rho_v + \mu} (\tilde{R}_{Cv}^a + \tilde{R}_{Cv}^s)}}, \quad (7)$$

where

$$R_{Cv}^a = \frac{b_v}{\delta + \rho_v + \mu} \cdot (1 - \sigma_v) \cdot \frac{\lambda}{\lambda + \mu} \cdot \frac{\beta_v}{d} \quad (8)$$

$$R_{Cv}^s = \frac{b_v}{\delta + \rho_v + \mu} \cdot \sigma_v \cdot \frac{\lambda}{\lambda + \mu} \cdot \frac{\nu_v}{\nu_v + \mu} \cdot \frac{\beta_v}{d}, \text{ and} \quad (9)$$

$\tilde{R}_{Cv}^i = R_{Cv}^i / \left(\frac{b_v \beta_v}{d(\delta + \rho_v + \mu)} \right)$, for $i = a, s$. Note that if δ were zero, in other words if *P. vivax* patients never relapsed, $R_{Cv} = \sqrt{R_{Cv}^a + R_{Cv}^s}$ where the interpretations of R_{Cv}^a and R_{Cv}^s are analogous to that of R_{Cf}^a and R_{Cf}^s , respectively. That is, R_{Cv}^a would be the contribution of an asymptomatic infectious individual to the basic reproductive number and R_{Cv}^s the contribution of a symptomatic infectious individual. However, the inclusion of the possibility of relapse in *P. vivax* infected individuals ($\delta > 0$) makes the expression for R_{Cv} more complicated and its biological interpretation less straight-forward. The numerator squared of R_{Cv} is the number of new mosquito infections arising from a single infected mosquito, without the intermediate human hosts relapsing.

To interpret the denominator of R_{Cv} , first note that $\tilde{R}_{Cv}^a + \tilde{R}_{Cv}^s \in [0, 1)$ since $\tilde{R}_{Cv}^a + \tilde{R}_{Cv}^s < \frac{\lambda}{\lambda + \mu} (1 - \sigma_v + \sigma_v) = \frac{\lambda}{\lambda + \mu} < 1$ and clearly $\tilde{R}_{Cv}^a + \tilde{R}_{Cv}^s$ is positive. Let $x = \frac{\delta}{\delta + \rho_v + \mu} (\tilde{R}_{Cv}^a + \tilde{R}_{Cv}^s)$. Then $x < 1$ implies that $\frac{1}{1-x} = \sum_{n=0}^{\infty} x^n$. Because $\frac{\delta}{\delta + \rho_v + \mu}$ is the probability that an individual in I_v relapses when there are no *falciparum*-infected individuals in the population, x is the probability that a liver-stage human will relapse. Thus, x^n is the probability that a liver-stage human will relapse n times. So,

$$R_{Cv}^2 = \sum_{n=0}^{\infty} (R_{Cv}^a + R_{Cv}^s) \cdot x^n. \quad (10)$$

The i^{th} term in the sum can be interpreted as the number of new mosquito infections generated by a single mosquito where the intermediate human hosts relapse exactly i times.

Since the only control measure explicitly implemented in the model is treatment, the basic reproductive number for the model is given by the control reproductive number evaluated with the treatment recovery rates (γ_v and γ_f) equal to the natural recovery rates (r_v and r_f , respectively). Using our definition of ρ_v , ρ_f , and δ this is equivalent to setting $\rho_v = r_v$, $\delta = r_v$, and $\rho_f = r_f$. Thus, $R_0 = \max\{R_{0v}, R_{0f}\}$, where

$$R_{0f} = \sqrt{\frac{\beta_f}{d} \cdot \left[(1 - \sigma_f) + \sigma_f \frac{\nu_f}{\nu_f + \mu} \right] \frac{b_f}{r_f + \mu}} \quad (11)$$

$$= \sqrt{R_{0f}^a + R_{0f}^s}, \quad (12)$$

where

$$R_{0f}^a = \frac{\beta_f}{d} \cdot (1 - \sigma_f) \cdot \frac{b_f}{r_f + \mu} \quad (13)$$

$$R_{0f}^s = \frac{\beta_f}{d} \cdot \sigma_f \cdot \frac{\nu_f}{\nu_f + \mu} \frac{b_f}{r_f + \mu}. \quad (14)$$

Similarly,

$$R_{0v} = \sqrt{\frac{\frac{b_v}{2r_v + \mu} \left(\tilde{R}_{0v}^a + \tilde{R}_{0v}^s \right) \frac{\beta_v}{d}}{1 - \frac{r_v}{2r_v + \mu} \left(\tilde{R}_{0v}^a + \tilde{R}_{0v}^s \right)}}, \quad (15)$$

where

$$\tilde{R}_{0v}^a = (1 - \sigma_v) \frac{\lambda}{\lambda + \mu} \quad (16)$$

$$\tilde{R}_{0v}^s = \sigma_v \frac{\lambda}{\lambda + \mu} \cdot \frac{\nu_v}{\nu_v + \mu}. \quad (17)$$

2.7 Isolated Endemic Equilibria and Coexistence

Determining an analytic expression for the coexistence equilibrium can be a difficult problem for more complicated models such as this two-parasite malaria model. However, we can still gain

insight into the conditions under which a coexistence equilibrium occurs by studying the stability of the isolated endemic equilibria; that is, the equilibria where only one pathogen is present in a population. Linearizing the system about these isolation equilibria provides a condition under which the absent parasite species can invade when introduced to the population. These threshold quantities are known as the invasion reproduction numbers.

First, we find the *vivax*-only equilibrium, \mathcal{E}_v by assuming all *falciparum*-infected variables are zero and setting each equation in the resulting system equal to zero. Solving this system of equations for the non-trivial equilibrium, we find that

$$j_v^* = \frac{b_v I_v^*}{b_v I_v^* + d\hat{K}} \quad (18)$$

$$S^* = \frac{\mu\hat{K} + \rho_v I_v^*}{\beta_v j_v^* + \mu} \quad (19)$$

$$L^* = \frac{\beta_v S^* j_v^* + \delta I_v^*}{\lambda + \mu} \quad (20)$$

$$C_v^* = \frac{\sigma_v \lambda}{\nu_v + \mu} L^*, \quad (21)$$

where

$$I_v^* = \frac{1 - R_{Cv}^2}{R_{Cv}^2} \cdot \frac{\mu\hat{K}}{\rho_v + \delta \left(1 - \frac{\delta + \rho_v + \mu}{\delta(R_{Cv}^a + R_{Cv}^s)}\right) \left(1 + \frac{\mu}{\beta_v}\right)} \quad (22)$$

It is simple to show that the denominator in equation (22) is always negative. First recall that $R_{Cv}^a + R_{Cv}^s < 1$ so that $\frac{\delta + \rho_v + \mu}{\delta(R_{Cv}^a + R_{Cv}^s)} > \delta + \rho_v + \mu$. So, $\rho_v + \delta \left(1 - \frac{\delta + \rho_v + \mu}{\delta(R_{Cv}^a + R_{Cv}^s)}\right) \left(1 + \frac{\mu}{\beta_v}\right) < \rho_v + \delta \left(1 - \frac{\delta + \rho_v + \mu}{\delta(R_{Cv}^a + R_{Cv}^s)}\right) < -\mu < 0$. The numerator of equation (22) is negative if $R_{Cv}^2 > 1$. Thus, I_v^* is positive only if $R_{Cv}^2 > 1$. In other words, the *vivax*-boundary equilibrium exists only when $R_{Cv} > 1$.

Now, we find the *falciparum*-only equilibrium \mathcal{E}_f by setting all *vivax*-infected variables equal to zero, and finding the non-trivial equilibrium of the resulting system.

$$j_f^* = \frac{b_f I_f^*}{b_f I_f^* + d\hat{K}} \quad (23)$$

$$S^* = \frac{\mu\hat{K} + \rho_f I_f^*}{\beta_f j_f^* + \mu} \quad (24)$$

$$C_f^* = \frac{\sigma_f \beta_f}{\nu_f + \mu} S^* j_f^*, \quad (25)$$

where

$$I_f^* = \frac{1 - R_{Cf}^2}{R_{Cf}^2} \cdot \frac{\mu\hat{K}}{\rho_f - \frac{b_f \beta_f}{d(R_{Cf}^a + R_{Cf}^s)} \left(1 + \frac{\mu}{\beta_f}\right)} \quad (26)$$

Using the definition of $R_{Cf}^a + R_{Cf}^s$, we have that $\frac{b_f \beta_f}{d(R_{Cf}^a + R_{Cf}^s)} = \frac{\rho_f + \mu}{(1 - \sigma_f) + \sigma_f \frac{\nu_f}{\nu_f + \mu}} < \rho_f + \mu$. Since $\rho_f - \frac{\rho_f + \mu}{(1 - \sigma_f) + \sigma_f \frac{\nu_f}{\nu_f + \mu}} (1 + \mu/\beta_f) < \rho_f - (\rho_f + \mu) = -\mu < 0$, the denominator of equation (26) is always negative. Consequently, I_f^* is positive only when $R_{Cf} > 1$.

2.8 Invasion numbers R_v^f and R_f^v

The basic reproduction number is a threshold that determines whether a disease can invade the disease-free equilibrium or not. Likewise, invasion numbers are threshold quantities that determine if a disease can invade another disease's endemic equilibrium. These quantities are very useful in understanding the competition between pathogens in a multi-strain model. Here, we find analytic expressions for R_v^f , the invasion number of *P. vivax* when the system is at the *P. falciparum*-only equilibrium, and R_f^v , the invasion number of *P. falciparum* at the *P. vivax*-only equilibrium. Typically, the following result can be established: if $R_{Cf} > 1$ and $R_v^f < 1$, then the *falciparum*-only equilibrium is locally asymptotically stable and unstable otherwise. Similarly, if $R_{Cv} > 1$ and $R_f^v < 1$, the *vivax*-only equilibrium is locally asymptotically stable and unstable otherwise. Both species coexist when R_v^f and R_f^v are greater than one.

The invasion numbers were derived using the next generation approach [11], the details of which are presented in appendix A.2. We find that

$$R_f^v = \left[\frac{1}{1 - k_{5,3} k_{6,5} k_{3,6}} \cdot (k_{2,1} k_{3,2} k_{1,3} + k_{2,1} k_{3,2} k_{5,3} k_{1,5} + k_{2,1} k_{3,2} k_{5,3} k_{6,5} k_{1,6} + k_{3,1} k_{1,3} + k_{3,1} k_{5,3} k_{1,5} + k_{3,1} k_{5,3} k_{6,5} k_{1,6} + k_{4,1} k_{6,4} k_{1,6} + k_{4,1} k_{6,4} k_{3,6} k_{1,3} + k_{4,1} k_{6,4} k_{3,6} k_{5,3} k_{1,5}) \right]^{1/2}. \quad (27)$$

The factor $1/(1 - k_{5,3}k_{6,5}k_{3,6})$ can be written as the geometric series $\sum_{n=0}^{\infty} (k_{5,3}k_{6,5}k_{3,6})^n$, where

$k_{5,3}k_{6,5}k_{3,6} = \frac{\alpha_f \beta_v j_v^*}{\alpha_f \beta_v j_v^* + \rho_f + \mu} \cdot \frac{\nu_{fv}}{\nu_{fv} + \mu} \cdot \frac{\eta_v}{\eta_v + \eta_f + \mu}$ is the probability that a *falciparum*-only infected human will loop through the path $I_f \rightarrow C_{fv} \rightarrow I_c \rightarrow I_f$ n times before infecting a mosquito. This loop arises when an I_f individual becomes co-infected, progresses to the I_c stage, and recovers from *vivax* malaria infection first, returning to the I_f stage. Note that an I_f individual can only transmit *P. falciparum* parasites by infecting a mosquito before leaving that stage, or by becoming co-infected and recovering first from *vivax* infection. Also note that $k_{5,3} = \frac{\alpha_f \beta_v j_v^*}{\alpha_f \beta_v j_v^* + \rho_f + \mu}$ is the transition probability for $I_f \rightarrow C_{fv}$, $k_{6,5} = \frac{\nu_{fv}}{\nu_{fv} + \mu}$ is the transition probability $C_{fv} \rightarrow I_c$, and finally $k_{3,6} = \frac{\eta_v}{\eta_v + \eta_f + \mu}$ represents the transition probability $I_c \rightarrow I_f$.

We can interpret the remaining terms in R_f^v similarly. Instead of a path representing a loop that a single individual takes, each path below represents the path for how one *falciparum* infected mosquito can lead to a new mosquito infection.

$$\begin{aligned}
k_{2,1}k_{3,2}k_{1,3} &= j_f \rightarrow C_f \rightarrow I_f \rightarrow j_f \\
k_{2,1}k_{3,2}j_{5,3}k_{1,5} &= j_f \rightarrow C_f \rightarrow I_f \rightarrow C_{fv} \rightarrow j_f \\
k_{2,1}k_{3,2}k_{5,3}k_{6,5}k_{1,6} &= j_f \rightarrow C_f \rightarrow I_f \rightarrow C_{fv} \rightarrow I_c \rightarrow j_f \\
k_{3,1}k_{1,3} &= j_f \rightarrow I_f \rightarrow j_f \\
k_{3,1}k_{5,3}k_{1,5} &= j_f \rightarrow I_f \rightarrow C_{fv} \rightarrow j_f \\
k_{3,1}k_{5,3}k_{6,5}k_{1,6} &= j_f \rightarrow I_f \rightarrow C_{fv} \rightarrow I_c \rightarrow j_f \\
k_{4,1}k_{6,4}k_{1,6} &= j_f \rightarrow C_{vf} \rightarrow I_c \rightarrow j_f \\
k_{4,1}k_{6,4}k_{3,6}k_{1,3} &= j_f \rightarrow C_{vf} \rightarrow I_c \rightarrow I_f \rightarrow j_f \\
k_{4,1}k_{6,4}k_{3,6}k_{5,3}k_{1,5} &= j_f \rightarrow C_{vf} \rightarrow I_c \rightarrow I_f \rightarrow C_{fv} \rightarrow j_f
\end{aligned}$$

If we multiply any one of the terms above by $\sum_{n=0}^{\infty} (k_{5,3}k_{6,5}k_{3,6})^n$, then the n^{th} term in the resulting sum will have the same chain of events as above, with the exception that the I_f individual takes the $I_f \rightarrow C_{fv} \rightarrow I_c \rightarrow I_f$ loop n times before continuing to the next stage in the chain. Thus, the next-generation approach leads to an expression of the invasion numbers whose square has the biological interpretation we desire: $\left(R_f^v\right)^2$ is the number of secondary *falciparum* mosquito infections caused by a single *falciparum*-infected mosquito in a population at the *vivax* isolated endemic equilibrium.

Now we introduce the invasion number R_v^f , whose expression is more complicated than that of R_f^v . Despite its more complicated form, we can show that the square of this invasion number is the number of new *vivax*-infected mosquitoes arising from a single *vivax*-infected mosquito in a population at the *falciparum* isolated endemic equilibrium. From the next generation approach, we

find that

$$\begin{aligned}
R_v^f = & \{[k_{6,1}(k_{1,5}k_{7,6}k_{4,7}(k_{5,4} + k_{2,4}k_{5,2}) + k_{1,7}k_{7,6}(1 - k_{2,4}(k_{3,2}k_{4,3} + k_{4,2}))) \\
& + k_{2,1}[(k_{1,5} + k_{1,7}k_{7,5})(k_{3,2}k_{4,3}k_{5,4} + k_{4,2}k_{5,4} + k_{5,2})]\} \\
& \div (1 - k_{2,4}(k_{3,2}k_{4,3} + k_{4,2}) - k_{4,7}k_{7,5}(k_{5,4} + k_{2,4}k_{5,2}))^{1/2}, \text{ where}
\end{aligned} \tag{28}$$

$$\begin{aligned}
k_{6,1} &= \frac{\alpha_f \beta_v I_f^*}{d} \\
k_{1,5} &= \frac{b_v(1 - j_f^*)}{\hat{K}(\nu_{vf} + \mu)} \\
k_{7,6} &= \frac{\nu_{vf}}{\nu_{vf} + \mu} \\
k_{4,7} &= \frac{\eta_f}{\eta_v + \eta_f + \mu} \\
k_{5,4} &= \frac{\alpha_v \beta_f j_f^*}{\alpha_v \beta_f j_f^* + \delta + \rho_v + \mu} \\
k_{2,4} &= \frac{\delta}{\alpha_v \beta_f j_f^* + \delta + \rho_v + \mu} \\
k_{5,2} &= \frac{\alpha_v \beta_f j_f^*}{\alpha_v \beta_f j_f^* + \lambda + \mu} \\
k_{1,7} &= \zeta k_{1,5} \\
k_{7,6} &= \frac{\nu_{fv}}{\nu_{fv} + \mu} \\
k_{3,2} &= \frac{\sigma_v \lambda}{\alpha_v \beta_f j_f^* + \lambda + \mu} \\
k_{4,3} &= \frac{\nu_v}{\nu_v + \mu} \\
k_{4,2} &= \frac{(1 - \sigma_v) \lambda}{\alpha_v \beta_f j_f^* + \lambda + \mu} \\
k_{2,1} &= \frac{\beta_v S^*}{d} \\
k_{7,5} &= \frac{\nu_{vf}}{\nu_{vf} + \mu}
\end{aligned}$$

To arrive at the correct biological interpretation, we first observe that expanding the expression for $(R_v^f)^2$ reveals that each term in the resulting sum represents a path by which one *vivax*-infected mosquito results in another mosquito infection. For example, the first term (rearranged),

$k_{6,1}k_{7,6}k_{4,7}k_{5,4}k_{1,5}$, represents the number of I_f -humans infected by a *vivax*-infected mosquito before dying, causing those humans to progress to the C_{fv} stage, times the fraction of people that survive the C_{fv} stage and progress to the I_c stage, times the fraction of individuals that survive this stage and are treated for *falciparum* prior to treatment for *vivax*, entering the I_v stage, times the probability that these individuals are infected by a *falciparum*-infected mosquito and progress to the C_{vf} stage, and finally, times the number of susceptible mosquitoes a C_{vf} human infects prior to progressing to the co-infectious stage I_c . Each term in R_v^f represents such a path from an infected mosquito to another mosquito infection. The negative terms, as we will demonstrate, account for infections that arise because a human passes through the same stage more than once. In appendix A.2, we argue that the denominator of R_v^f is positive. Thus, it must be that $k_{2,4}(k_{3,2}k_{4,3} + k_{4,2}) + k_{4,7}k_{7,5}(k_{5,4} + k_{2,4}k_{5,2})$ is less than one. Using the same reasoning as we did for R_{Cv} and R_f^v , we can rewrite $1/(1 - k_{2,4}(k_{3,2}k_{4,3} + k_{4,2}) - k_{4,7}k_{7,5}(k_{5,4} + k_{2,4}k_{5,2}))$ as a geometric series, allowing us to fully interpret the invasion number.

Since $1/(1 - x - y) = \sum_{n=0}^{\infty} (x + y)^n$ when $|x + y| < 1$, we can rewrite R_v^f as

$$\begin{aligned} \left(R_v^f\right)^2 &= \left[k_{6,1}k_{1,5}k_{7,6}k_{4,7}(k_{5,4} + k_{2,4}k_{5,2}) \right. \\ &\quad \left. + k_{2,1}(k_{1,5} + k_{1,7}k_{7,5})(k_{3,2}k_{4,3}k_{5,4} + k_{4,2}k_{5,4} + k_{5,2}) \right] \\ &\quad \times \sum_{n=0}^{\infty} [k_{2,4}(k_{3,2}k_{4,3} + k_{4,2}) + k_{4,7}k_{7,5}(k_{5,4} + k_{2,4}k_{5,2})]^n \\ &\quad + k_{6,1}k_{1,7}k_{7,6} \frac{1 - k_{2,4}(k_{3,2}k_{4,3} + k_{4,2})}{1 - k_{2,4}(k_{3,2}k_{4,3} + k_{4,2}) - k_{4,7}k_{7,5}(k_{5,4} + k_{2,4}k_{5,2})} \end{aligned} \quad (29)$$

Now, we can rewrite the fraction in the last term so that the expression for R_v^f is fully interpretable. Note that this term is of the form $(1 - x)/(1 - x - y)$, where x is precisely $k_{2,4}(k_{3,2}k_{4,3} + k_{4,2})$ and y is $k_{4,7}k_{7,5}(k_{5,4} + k_{2,4}k_{5,2})$. Using the fact that $\frac{1-x}{1-x-y} = \frac{1-x-y+y}{1-x-y} = 1 + \frac{y}{1-x-y}$, we have that

$$\frac{1 - x}{1 - x - y} = 1 + y \sum_{n=0}^{\infty} (x + y)^n \quad (30)$$

Hence, we arrive at a fully interpretable expression for the invasion number

$$\begin{aligned} \left(R_v^f\right)^2 &= \left[k_{6,1}k_{1,5}k_{7,6}k_{4,7}(k_{5,4} + k_{2,4}k_{5,2}) \right. \\ &\quad \left. + k_{2,1}(k_{1,5} + k_{1,7}k_{7,5})(k_{3,2}k_{4,3}k_{5,4} + k_{4,2}k_{5,4} + k_{5,2}) \right] \\ &\quad \times \sum_{n=0}^{\infty} (x + y)^n + k_{6,1}k_{7,6}k_{1,7} \left(1 + y \sum_{n=0}^{\infty} (x + y)^n \right). \end{aligned} \quad (31)$$

The terms $x = k_{2,4}(k_{3,2}k_{4,3} + k_{4,2})$ and $y = k_{4,7}k_{7,5}(k_{5,4} + k_{2,4}k_{5,2})$ represent four different transmission paths. x represents two ways a person can start in, and return to, stage I_v . One path travels through the symptomatic class while the other does not. Similarly, y represents two ways in which a person in I_c can arrive at stage C_{vf} . One of these two paths travels through stage L , while the other path bypasses stage L .

The n^{th} term in the summation $\sum_{n=0}^{\infty} (x+y)^n$ represents the probability of taking any combination of the four loops, resulting in a total of exactly n loops. The 1 in parentheses represents the probability that an individual makes no loops. Finally, the n^{th} term in the expression $y \sum_{n=0}^{\infty} (x+y)^n$ represents the probability that an individual first takes one of the loops in y , then makes a total of exactly n loops consisting of some combination of the four loops described by x and y . The second summation in equation (31) arises because the only way in which an individual can enter path x ($I_v \rightarrow L(L \rightarrow C_v \rightarrow I_v + L \rightarrow I_v)$) from path $k_{1,7}k_{6,1}k_{7,6}$ ($I_c \rightarrow j_v \rightarrow C_{fv} \rightarrow I_c$) is by first entering path y ($I_c \rightarrow I_v(I_v \rightarrow C_{vf} + I_v \rightarrow L \rightarrow C_{vf})$). Conversely, paths x and y can be reached from all other paths represented in equation (31).

By carefully rewriting the invasion numbers to consist of terms that can be interpreted as either probabilities or fractions of a population of individuals in a particular state, we have shown that it is possible to link the mathematical expressions to a biological interpretation relevant to public health. In Section 3.4, we illustrate how these analytic expressions can be used to understand the interplay between the use of malaria interventions and the competition between *falciparum* and *vivax*.

3 Description of model parameters and choice of parameter values for the years from 1987 to 1996

To answer questions about disease dynamics and the use of control measures in India, we must determine realistic estimates to parameterize our mathematical model. To do this we found reasonable estimates from the malaria literature for all parameters but the transmission parameters (b_v, b_f, β_v , and β_f) and human population growth parameters (r and K). Using these estimates from the literature, we estimate the remaining parameters by fitting the model to malaria case data for India. In the following sections we first discuss the choice of estimates for parameters found in the literature, then we describe the procedure for estimating the human population intrinsic growth rate, carrying capacity, and the malaria transmission parameters.

Table 2: Description of model parameters pertaining to mosquito population dynamics and their estimates

Parameters	Description	Value	Reference
d	Natural death rate	$\frac{365}{14} \text{ years}^{-1}$	[3]
ζ	Probability that a susceptible mosquito that gets infected by a co-infected human contracts <i>P. vivax</i>	$\frac{670}{670+332}$	see 3.1.4
$1 - \zeta$	Probability that a susceptible mosquito that gets infected by a co-infected human contracts <i>P. falciparum</i>		

3.1 Estimation of parameters from literature

3.1.1 Time to infectiousness

Following the onset of symptoms, it takes roughly 4 days for *P. vivax* infections to become infectious in a human host [12], and approximately 7 days for *P. falciparum* infection [18]. Thus, we take ν_v and ν_f , the rate of progression from symptomatic to infectious for *P. vivax* and *P. falciparum*, respectively, to be $\frac{365}{4} \text{ years}^{-1}$ for *P. vivax*, and $\frac{365}{7} \text{ years}^{-1}$ for *P. falciparum*. We assume that becoming co-infected does not alter the time it takes to become infectious. Thus, we let $\nu_{fv} = \nu_v$ and $\nu_{vf} = \nu_f$.

3.1.2 Estimating recovery rates

The rate of recovery from I_v and I_f to the susceptible class S is estimated by $\rho_v = (1 - \sigma_v)r_v + \sigma_v\gamma_v$ and $\rho_f = (1 - \sigma_f)r_f + \sigma_f\gamma_f$, respectively. In other words, a fraction recover at the natural recovery rate, and a fraction recover at the treatment recovery rate. Since Chloroquine targets only the asexual blood stages of the parasite, there may still be gametocytes remaining at the end of treatment. It takes roughly 8 days for gametocytes to mature, and the lifespan of a mature gametocyte is roughly between 3.5 and 4 days. From this, we estimate that individuals treated for *falciparum* with drugs that do not kill the gametocytes can remain infectious for up to 12 (8+4) days after treatment is completed. Thus, treatment of *P. falciparum* infections with Chloroquine reduces the infectious period from roughly 200 days (ref) to 12 days, and we take $r_f = \frac{365}{200} \text{ years}^{-1}$, and $\gamma_f = \frac{365}{12} \text{ years}^{-1}$. A study of *P. vivax* gametocytemia found that out of 516 patients treated with CQ, only 4 still had not cleared the gametocytes by the third day of treatment [22]. Using this finding, we let $\gamma_v = \frac{365}{3}$.

Table 3: Description of model parameters pertaining to human population dynamics and their estimates

Parameters	Description	Value	Reference
$\frac{1}{\lambda}$	Duration of <i>P. vivax</i> liver stage	90 days	see 3.1.3
$\frac{1}{\nu_v}$	Time until infectious after <i>P. vivax</i> symptom onset	4 days	[12]
$\frac{1}{\nu_f}$	Time until infectious after <i>P. falciparum</i> symptom onset	7 days	[18]
$\frac{1}{\nu_{vf}}$	Duration of C_{vf}	$\frac{1}{\nu_f}$	see 3.1.1
$\frac{1}{\nu_{fv}}$	Duration of C_{fv}	$\frac{1}{\nu_v}$	see 3.1.1
μ	Natural death rate	$\frac{1}{60.55}$ years ⁻¹	see 3.3
γ_v	<i>P. vivax</i> blood-stage parasite clearance rate with treatment	$\frac{1}{3}$ days ⁻¹	[24]
γ_f	<i>P. falciparum</i> treatment recovery rate	$\frac{1}{12}$ days ⁻¹	see 3.1.2
r_v	<i>P. vivax</i> natural blood-stage parasite clearance rate	365/30 years ⁻¹	see 3.1.3
r_f	<i>P. falciparum</i> natural recovery rate	$\frac{365}{200}$ years ⁻¹	see 3.1.2
ρ_v	Recovery rate from I_v to S		see 3.1.2
ρ_f	Recovery rate from I_f to S		see 3.1.2
p_r	Probability of post-treatment <i>P. vivax</i> relapse	0.23 – 0.44 (0.2904)	[1]
δ	<i>P. vivax</i> relapse rate	$p_r \sigma_v \gamma_v + (1 - \sigma_v)r_v$	see 3.1.3
σ_v	Probability that a <i>P. vivax</i> infected human becomes symptomatic	0.82	[29]
σ_f	Probability that a <i>P. falciparum</i> infected human becomes symptomatic	0.90	assumed
α_v	<i>Pv</i> -induced cross-immunity to <i>Pf</i>	1	
α_f	<i>Pf</i> -induced cross-immunity to <i>Pv</i>	1	
η	Fraction of co-infected infectious individuals that recover first from <i>P. falciparum</i>	0.75	see 3.2
η_v	Rate of progression from I_c to I_f due to <i>P. vivax</i> treatment	$\eta \gamma_v$	
η_f	Rate of progression from I_c to I_v due to <i>P. falciparum</i> treatment	$(1 - \eta) \gamma_f$	

3.1.3 Parameterizing *P. vivax* relapse

Joshi et al. [16] note that patterns of *P. vivax* relapse can be categorized into three groups. The first group is referred to as the tropical type which is characterized by an early primary attack with frequent relapses. The time intervals between relapses of the tropical type are between one and three months. Group II has relapse intervals of intermediate length - approximately between three and five months long. And finally, group III, also known as the temperate type, is characterized by a long primary latent period and relapses occurring every six to seven months.

In this malaria model, we assume that *P. vivax* infected individuals who relapse are those who either were never treated or were unsuccessfully treated. Since *P. vivax* parasites inducing short-term relapse patterns were found to be less susceptible to anti-relapse drugs [16], we assume that individuals who were unsuccessfully treated for *P. vivax* exhibit group I relapse patterns. Thus, they should relapse every one to three months. The rate at which a relapsing individual progresses from I_v to L is the rate at which that individual loses infectiousness (i.e. the rate at which gametocytes are cleared from the blood). We assume that treated individuals lose infectiousness at a rate γ_v , regardless of whether treatment was successful or not, and untreated (i.e. asymptomatic) individuals lose infectiousness at a rate r_v . Adak et al. determined that 29.04 percent of *P. vivax* patients treated only with Chloroquine (CQ) relapsed following treatment [1]. Thus, the rate at which individuals progress from I_v to the liver stage class L , is given by $\delta = .2904\sigma_v\gamma_v + (1 - \sigma_v)r_v$. If no one is treated, then $\delta = r_v$.

The time between *P. vivax* relapses is usually defined as the time between clinical episodes. However, in this model it is possible for individuals who relapse, in the sense that the parasite repeats the cycle of infection within the human host, without passing through the symptomatic stage C_v . We will take the time between relapses to be the time it takes to progress from I_v to L ($\frac{1}{r_v}$ for an untreated individual and $\frac{1}{\gamma_v}$ for an unsuccessfully treated individual), plus the time it takes to progress from L to the next infected stage ($\frac{1}{\lambda}$). Thus, if we take the average time between relapses to be three months for an unsuccessfully treated individual, $\frac{1}{\lambda} + \frac{1}{\gamma_v} = 3$ months $\approx 90 - 93$ days. Since $\frac{1}{\gamma_v}$ is approximately 3 days long, we take $\frac{1}{\lambda}$ to be 90 days. In other words, $\lambda = \frac{365}{90}$ years⁻¹. Asymptomatic individuals could have relapse patterns associated with group I, II, or III - experiencing a relapse anywhere from every one to seven months. Thus, we take $\frac{1}{r_v} + \frac{1}{\lambda}$ to be the average of four months long. In other words, $\frac{1}{\lambda} + \frac{1}{r_v} \approx 120 - 124$ days. From this estimate and our estimate for $1/\lambda$, we assume that it takes roughly 30 days for an untreated *P. vivax* infected individual to lose infectiousness.

3.1.4 Estimation of ζ

A study conducted by Phimpraphi et al. [25] showed no significant difference in gametocyte production by *P. vivax* or *P. falciparum* parasites in a co-infected human than in humans who were

only infected with one of the two parasite species. Also, *P. vivax* gametocyte densities were found to be higher than *P. falciparum* densities in infected humans, with roughly 670 *P. vivax* gametocytes per μl of blood and 332 *P. falciparum* gametocytes per μl of blood. Since gametocytes are the infectious stage of the malaria parasites in humans, we use these findings to determine a rough estimate of the parameter ζ , the proportion of mosquitoes infected by a human in I_c that contract *P. vivax*. We assume that ζ is the density of *vivax* gametocytes in the blood divided by the total gametocyte density. In other words, $\zeta = \frac{670}{670+332} \approx 0.67$.

3.2 Estimation of η

P. vivax and *P. falciparum* are also endemic to Thailand with roughly half the cases resulting from *P. vivax* infection and half due to *P. falciparum* infection. Approximately 10 percent of cases in Thailand initially diagnosed as *P. vivax* cases and 30 percent of cases initially diagnosed as *P. falciparum* cases turned out to be co-infections [33]. From this, we estimated that the proportion of co-infected cases treated first for *P. falciparum* is $\eta = 0.75$.

3.3 Estimation of population growth and transmission parameters using population and malaria case data for India

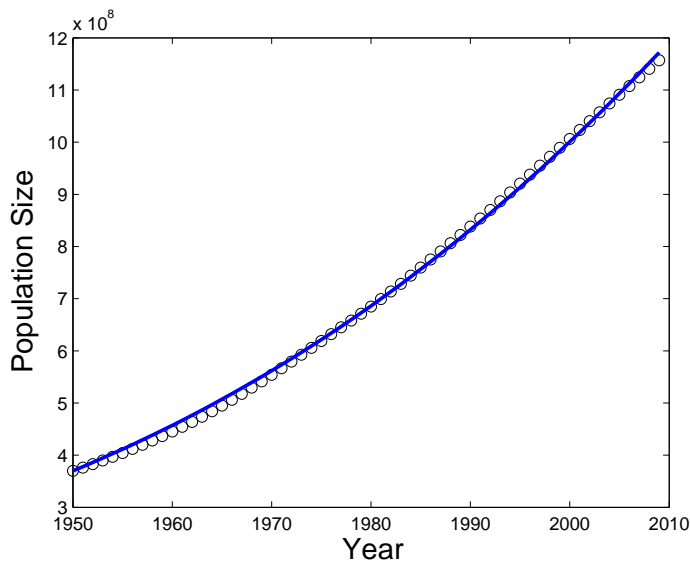


Figure 2: Plot of time series data for India's Population Size from 1950 to 2009 and the best fit of the logistic curve to this data. Population data was obtained from [28].

From life expectancy data for India [19], we estimated that the average life expectancy between the years 1987 and 2009 is approximately 60.55 years, giving us $\mu = 1/60.55 \text{ years}^{-1}$. Using this estimate and a nonlinear least-squares fit of the logistic equation to India’s population data, estimates are obtained for the parameters r and K (see Table 4). The best fit of the logistic curve is illustrated in Figure 2.

Table 4: Estimates of r and K .

Parameter	Description	Estimate	CI
r	Intrinsic growth rate	0.0398 years^{-1}	0.0392–0.0404
K	Population Carrying capacity	$7.5616 \cdot 10^9$ humans	$6.2919 \cdot 10^9$ – $8.8313 \cdot 10^9$

Assuming that the use of control measures remained fairly similar during the period from 1987 to 1996, we can estimate the transmission rates $b_v, b_f, \beta_v, \beta_f$ by imputing the parameter values in Tables 2, 3, and 4, and fitting the model to the malaria case data. More precisely, we used the ‘nlinfit’ function in MATLAB to minimize the sum of squares of the difference between the data and the solutions curves by comparing solution curve C_v to the *P. vivax* data and similarly comparing the solution curve $C_f + C_{vf} + C_{fv}$ to the *P. falciparum* plus mixed-case data. From this fitting procedure, we obtain estimates for the transmission parameters, summarized in Table 5. The controlled reproduction numbers R_{Cv} and R_{Cf} can now be calculated using the expressions in Section 2.5 (see Table 5).

Table 5: Pre-1997 estimates of the transmission parameters.

Parameter	Estimate	CI
b_v	14.5409	14.2907–14.7911
b_f	14.0442	6.2573–21.8311
β_v	191.3306	188.3507–194.3105
β_f	51.7312	23.2618–80.2006
R_{Cv}	1.0203	
R_{Cf}	1.0052	

The resulting reproduction number is larger than one, implying mathematically that at least one of the two malaria parasites will persist. Yet, in practice, the extremely close proximity of R_{Cv} and R_{Cf} to the persistence threshold makes it difficult to arrive at any definitive conclusion regarding the outcome of malaria in India. As a step towards addressing this concern, we use a parametric bootstrapping procedure to estimate confidence intervals for R_{Cv} and R_{Cf} . The procedure, which we will re-iterate here with slight modifications, is described in [8] by Chowell et al.

Let us denote the solution curves C_v and $C_f + C_{fv} + C_{vf}$ that best fit the data by S_v and S_f , respectively. In one iteration of the bootstrap procedure, we simulate new *vivax* case data by

Table 6: Pre-1997 mean, median, standard deviations, and confidence intervals for R_{Cv} and R_{Cf} , derived from parametric bootstrap.

Parameter	mean	median	stand. dev.	95% CI
R_{Cv}	1.0203	1.0204	0.0006	1.0192–1.0214
R_{Cf}	1.0052	1.0052	0.0001	1.005–1.0055

drawing points for each year (1987-1996) from a Poisson distribution with mean equal to the value of S_v at the corresponding year. In the same iteration we simulate new *falciparum*/mixed case data in the same manner. New estimates for the transmission parameters are determined by fitting C_v and $C_f + C_{fv} + C_{vf}$ to the simulated data. This procedure is repeated 1000 times. Calculating the isolated controlled reproduction numbers for each of the 1000 runs allows us to produce histograms of the 1000 values of R_{Cv} and R_{Cf} . These figures (see Figures 3) reveal that the values of the reproduction numbers generated by the bootstrapping procedure appear fairly symmetric. Consequently, it is simple to determine appropriate 95% confidence intervals for R_{Cv} and R_{Cf} (see Table 6) by determining the 0.025 and 0.975 quantiles of the 1000 estimates. Figure 3 illustrates that the estimates of R_{Cv} , R_{Cf} , R_v^f , and R_f^v are consistently greater than one. Hence, we can conclude that the two *Plasmodium* species would likely continue to coexist after 1997 had malaria intervention strategies not improved.

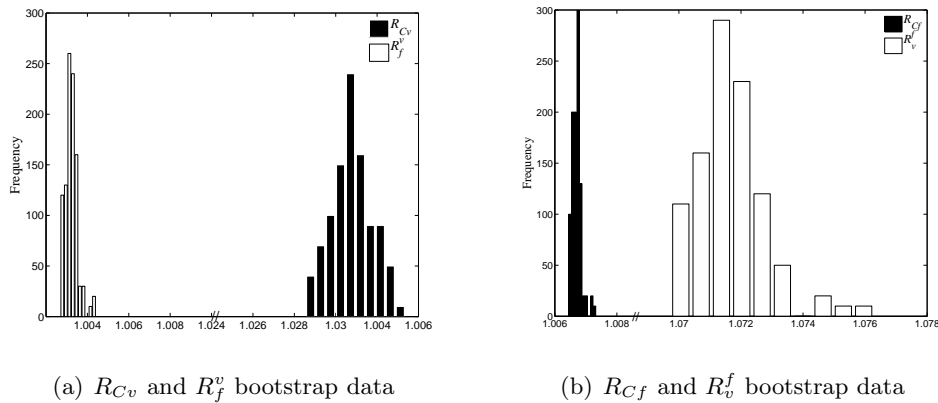


Figure 3: Histograms of (a) R_{Cv} and R_f^v data and (b) R_{Cf} and R_v^f data generated by bootstrap for the period 1987-1996.

3.4 Estimation of parameters for the enhanced malaria control period

Around 1997, several programs arose that resulted in an upsurge in funding for malaria control in India. As a consequence of enhanced malaria control, parameters related to different control policies undoubtedly also changed around 1997. Here, we attempt to assess that change by again fitting our malaria model, this time to case data for the period 1997-2010.

In general, an increase in the use of bednets decreases mosquito biting rate, increased use of insecticide treated bednets (ITNs) both decreases biting rate and increases the mosquito mortality rate, improved treatment increases the recovery rate, and insecticides increase the mosquito mortality rate. A combination of these control measures is often used. Our first goal here is to understand which of these control measures, or combination of control measures, contributed the most to the decline in the number of malaria cases after 1996. Secondly, we want to understand how the increase in funding for malaria has affected the competition between *P. vivax* and *P. falciparum*.

To address the first question – which parameters contributed the most to the post-1996 decline in cases – we fit the model to the 1997-2010 data several times, each time estimating a different combination of parameters relevant to malaria control while leaving the remaining parameters in the model fixed to their 1987-1996 estimates. We consider each of these parameterizations of the model to be a different model. For each model, we calculate the corrected Akaike Information Criterion (AICc) - a measure of the goodness of fit of a model to the data, discounted by the number of parameters estimated relative to the size of the dataset. The AICc values allow us to order the models from best to worst: the model with the smallest AICc is the best model, and the model with the largest AICc is the worst model. To make the distinction between the models clearer, we calculate the ΔAICc for each model: the difference in AICc between the model and the model with the smallest AICc. This means that the “best” model has a ΔAICc of zero. The results of this model comparison are summarized in Table 7. The rule of thumb is that candidate models with ΔAICc ’s between 0 and 2 have strong support, models with ΔAICc between 4 and 7 have considerably less support (but should still be considered), and models with ΔAICc greater than 10 should be disregarded as potential candidates [5].

The results of this analysis yielded that model $\mathcal{A} = \{\gamma_v, \gamma_f, a_v, a_f\}$ corresponding to estimating treatment recovery rate and biting rate parameters best explains the observed data. Using the rule of thumb for ΔAICc values, model \mathcal{B} has strong support, models \mathcal{C} , \mathcal{D} , \mathcal{E} , and \mathcal{F} have less support but should still remain in the pool of possible models, and model \mathcal{G} should be discarded. However, it is important to point out that models \mathcal{A} and \mathcal{B} were sensitive to the initial guess for the parameter values in the fitting procedure, whereas the remaining model results were fairly robust to the initial guess. This means that the relationship between models \mathcal{C} , \mathcal{D} , \mathcal{E} , \mathcal{F} , and \mathcal{G} remain the same for different initial parameter guesses while \mathcal{A} and \mathcal{B} find different positions in the list depending on the initial guess. We arrived at the ordering presented in Table 7 by repeating the fitting procedure for 3 different initial guesses for each of the seven models, and choosing the estimates corresponding to the smallest confidence intervals.

In general, adding the estimation of d , mosquito death rate, to a model increased the AICc value, suggesting that changes in mosquito death rate do not explain the decline in cases beginning in 1997. Similarly, since model $\mathcal{C} = \{a_v, a_f\}$ performed better than $\mathcal{D} = \{\gamma_v, \gamma_f\}$ and likewise $\mathcal{E} = \{a_v, a_f, d\}$ performed better than $\mathcal{F} = \{\gamma_v, \gamma_f, d\}$, we conclude that changes in mosquito biting rate better explain the decline in malaria prevalence than do changes in treatment recovery rates. Moreover, a smaller change in biting rate (roughly half) is required to yield the same results as changing the treatment recovery rate.

Some of the results are more surprising and difficult to interpret. For example, the results of model \mathcal{A} suggest that treatment recovery rates in 1997-2010 were worse, particularly for treatment of *vivax* malaria, than in 1987-1996. This outcome of the model could be a consequence of increased parasite resistance to drugs.

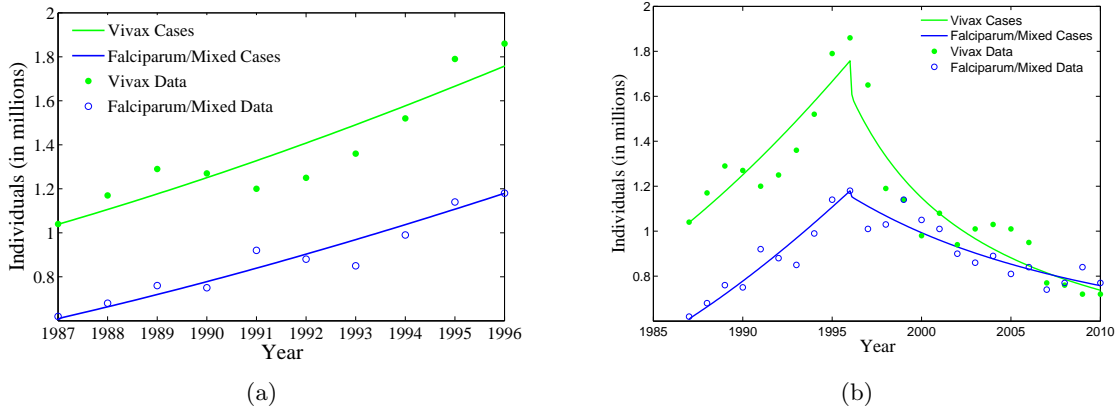


Figure 4: (a) Best fit of model to 1987-1996 case data; (b) Best fit of model to 1997-2010 data. Data from [9].

Models \mathcal{A} through \mathcal{F} can also provide some insight into how enhanced control measures affect the competition between *P. falciparum* and *P. vivax*. Using the parameter estimates yielded by each candidate model and the analytic expressions for the reproduction numbers R_{Cv} and R_{Cf} along with analytic expressions for the invasion numbers R_v^f and R_v^v , we can determine in which region of the competitive outcome graph the point $\{R_{Cv}, R_{Cf}\}$ lies. The set of candidate models $\{\mathcal{A}, \mathcal{B}\}$ yields a set of reproduction numbers lying in a region where *P. vivax* outcompetes *P. falciparum* (Figure 5). On the other hand, the set of models $\{\mathcal{C}, \mathcal{D}, \mathcal{E}, \mathcal{F}\}$ yields a set of reproduction numbers lying within corresponding invasion boundaries where *P. falciparum* outcompetes *P. vivax*. A summary of the isolation reproduction numbers resulting from each model candidate is given in Table 8. The result that model \mathcal{A} predicts *P. vivax* will outcompete *P. falciparum* is surprising given that the data suggests the opposite. However, extending the solution corresponding to model \mathcal{A} (Figure 6) to the year 2200 confirms that the data is potentially misleading. Although the proportion of cases due to *falciparum* has been increasing, model \mathcal{A} reveals that this observation is insufficient to draw

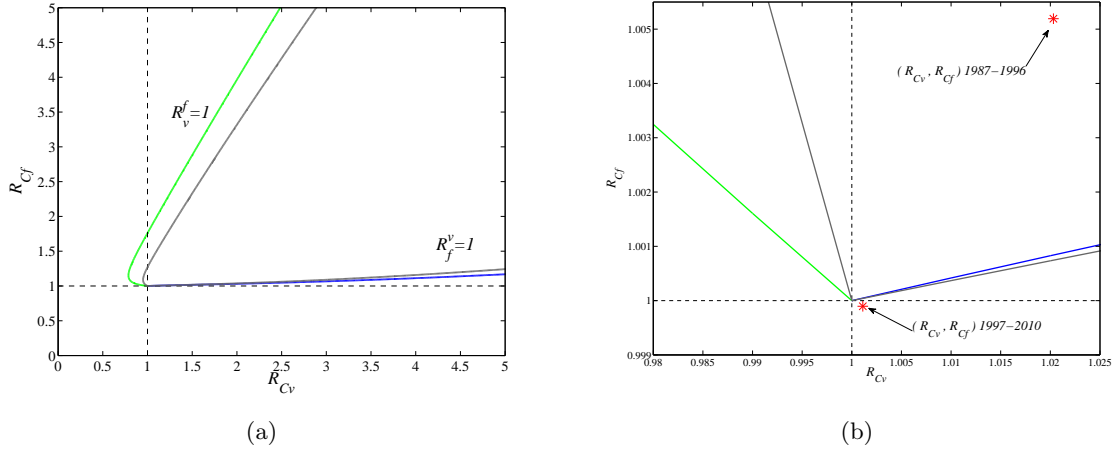


Figure 5: (a) Graph of $R_v^f = 1$ and $R_f^v = 1$ for the period 1987-1996 (green and blue lines, respectively) and 1997-2010 (grey lines) as a function of R_{Cv} and R_{Cf} ; (b) Plot of the point (R_{Cv}, R_{Cf}) for India before and after 1997. Prior to 1997, India was in the coexistence region. During period of enhanced control measures (1997-2010), India is in the region where *P. vivax* will eventually outcompete *P. falciparum*.

conclusions about the longterm competitive outcome of the two species.

While this type of analysis has the potential to unveil information regarding the future of malaria in a region, the reproduction numbers in each case lie very close to the invasion boundaries, and consequently it is difficult to draw definitive conclusions about the outcome of malaria. To address this concern, we again carried out a parametric bootstrap procedure to not only estimate confidence intervals for the reproduction numbers, but to also determine what the probability is that the reproduction number will lie in any one of the four possible competitive-outcome regions. For each of the six candidate models, we also calculated the AICc for every 1000 runs in the bootstrap routine to determine what the most frequent ordering of the set of candidate models is. To make sure that the results of the bootstrap method between models is comparable, we draw 1000 sets of data from a Poisson distribution with mean equal to the solution curve associated with model \mathcal{A} in Table 7 – the best fitting model based on AICc values.

The bootstrapping procedure allowed us to compile 1000 sets of parameter estimates for each of the six models (ignoring model \mathcal{G} because of the poor fit), from which we computed 1000 pairs of reproduction numbers (R_{Cv}, R_{Cf}) . The new parameter sets and reproduction number pairs were used to compute the invasion numbers for the 1000 runs, allowing us to determine what the probability is that a model will land in a particular competitive-outcome region. The results are listed in Table 9. The competitive outcomes vary the most for models \mathcal{A} and \mathcal{B} , which is consistent with our earlier observation that these two models were the most sensitive to the initial parameter

Table 7: Post-1996 models ordered by $\Delta AICc$ value (difference from best AICc value -123.9).

Model	Parameter	Percent change from pre-1997 estimate	CI	$\Delta AICc$
\mathcal{A}	a_v	-43.3	-67.3 – -19.3	0.0
	a_f	-1.1	-1.2 – -1.1	
	γ_v	-68.1	-97.4 – -38.8	
	γ_f	-1.2	-1.5 – -0.9	
\mathcal{B}	a_v	-45.4	-67.9 – -22.9	2.8
	a_f	0.9	-7.9 – 9.8	
	γ_v	-73.3	-97.4 – -49.2	
	γ_f	-5.9	-22.6 – 10.8	
	d	9.4	9.2 – 9.5	
\mathcal{C}	a_v	-3.1	-3.3 – -2.9	4.1
	a_f	-0.5	-0.5 – -0.5	
\mathcal{D}	γ_v	6.9	6.8 – 7.0	5.2
	γ_f	1.0	0.9 – 1.1	
\mathcal{E}	a_v	-0.6	-0.8 – -0.4	7.0
	a_f	2.0	2.0 – 2.1	
	d	5.2	5.1 – 5.2	
\mathcal{F}	γ_v	3.7	3.5 – 3.8	7.1
	γ_f	-1.9	-2.4 – -1.4	
	d	2.9	2.4 – 3.4	
\mathcal{G}	d	2.4	1.8 – 3.0	85.7

guess used for fitting.

Although the 1000 bootstrapped samples resulted in 123 different orderings, 5 orderings made up more than half of the samples. The original ordering $\{\mathcal{A}, \mathcal{B}, \mathcal{C}, \mathcal{D}, \mathcal{E}, \mathcal{F}, \mathcal{G}\}$ occurred 10.1% of the time. 29.5% of the runs led to the ordering $\{\mathcal{A}, \mathcal{C}, \mathcal{D}, \mathcal{E}, \mathcal{F}, \mathcal{B}, \mathcal{G}\}$. 9.7% of the samples yielded the ordering $\{\mathcal{C}, \mathcal{D}, \mathcal{E}, \mathcal{F}, \mathcal{A}, \mathcal{B}, \mathcal{G}\}$. The ordering $\{\mathcal{C}, \mathcal{D}, \mathcal{E}, \mathcal{F}, \mathcal{B}, \mathcal{A}, \mathcal{G}\}$ appeared 8.4% of the time, while 4.7% of the samples resulted in the ordering $\{\mathcal{B}, \mathcal{A}, \mathcal{C}, \mathcal{D}, \mathcal{E}, \mathcal{F}, \mathcal{G}\}$. The AICc values selected model \mathcal{A} as the top model 54.4% of the time. Of these 544 samples for which model \mathcal{A} was selected as the top model, roughly 15.1% yielded the outcome that *vivax* and *falciparum* would continue to coexist, 44.9% yielded that *vivax* would outcompete *falciparum*, 18.4% yielded that *falciparum* would outcompete *vivax*, and finally 21.7% yielded that both species would become extinct.

Determining confidence intervals for the reproduction numbers for each model was not as straightforward as it was for the 1987-1996 time period. Histograms of the reproduction numbers for each model revealed that not all of the samples of R_{Cf} were symmetric. In fact, the collection of

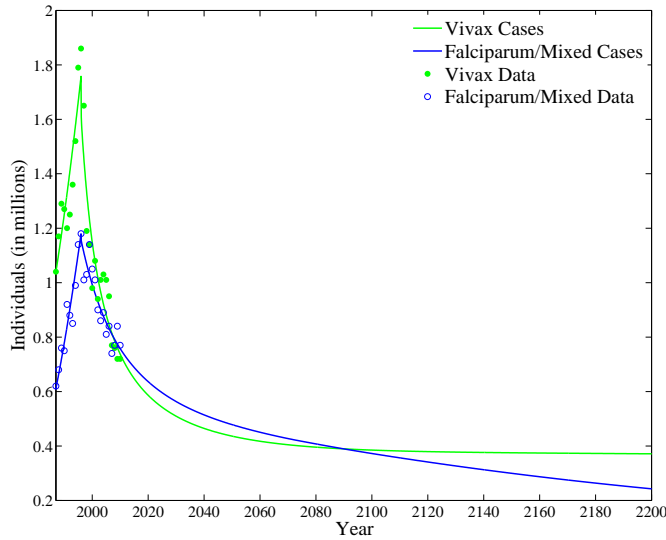


Figure 6: Model \mathcal{A} solution curve extended to the year 2200.

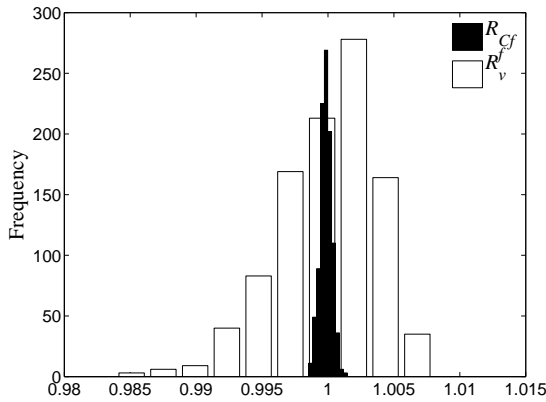
Table 8: 1997-2010 estimates of R_{Cv} and R_{Cf} for each candidate model.

	\mathcal{A}	\mathcal{B}	\mathcal{C}	\mathcal{D}	\mathcal{E}	\mathcal{F}
R_{Cv}	1.00111	1.00221	0.98891	0.98757	0.98874	0.98820
R_{Cf}	0.99990	0.99997	1.00018	1.00014	1.00015	1.00022

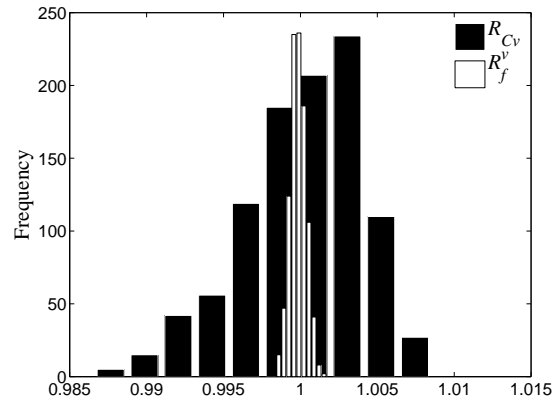
reproduction numbers R_{Cf} for model \mathcal{B} exhibits a bimodal distribution. Since, models \mathcal{A} and \mathcal{C} were the most common models taking “first place”, and because their corresponding reproduction numbers exhibited fairly symmetric distributions (see Figure 7), we present the confidence intervals for these two models. The 95% confidence intervals for R_{Cv} and R_{Cf} , respectively, corresponding to model \mathcal{A} are (0.99133 – 1.00640) and (0.99890 – 1.00075). For model \mathcal{C} , the confidence intervals are (0.98676 – 0.99079) and (0.99979 – 1.00054). Ultimately, the percentages in Table 9 provide more meaningful information than the confidence intervals derived for the post-1996 reproduction numbers. Figure 7 illustrates that the spread of the R_{Cf} data resulting from the bootstrap procedure was always less than the spread of R_v^f . Conversely, the variance in R_{Cv} is greater than that of R_f^v . This observation, which was consistent across all six candidate models suggests that R_{Cf} is less sensitive than R_v^f , and R_{Cv} is more sensitive than R_f^v , to changes in parameter values.

Table 9: Percentage of bootstrap runs in which *vivax* and *falciparum* will coexist (I), *vivax* will outcompete *falciparum* (II), *falciparum* will outcompete *vivax* (III), and the percentage of runs in which both will become extinct (IV).

	I	II	III	IV
\mathcal{A}	14.3	44.0	19.2	22.5
\mathcal{B}	4	11.3	53.3	31.4
\mathcal{C}	0.2	0	77.4	22.4
\mathcal{D}	0	0	74.3	25.7
\mathcal{E}	0	0	77.9	22.1
\mathcal{F}	0.4	0	83.40	16.2



(a) Model \mathcal{A} R_v^f, R_{Cf} data



(b) Model \mathcal{A} R_f^v, R_{Cv} data

Figure 7: Subfigure (a) presents a histogram of the R_v^f and R_{Cv} bootstrap data for model \mathcal{A} . Subfigure (b) is a histogram of the R_f^v and R_{Cf} bootstrap data for model \mathcal{A} .

4 Discussion

India, as is true for many other countries, has struggled with the control of malaria, experiencing several ups and downs. While more recent efforts have been successful in dramatically decreasing the number of cases, India is still far from reaching its goal. Consequently, knowing which of the control strategies India's success can be attributed to is valuable to India's future success and could help India use their resources more efficiently. The presence of two malaria parasites in India makes this a challenging problem, both in practice and in terms of mathematical modeling. To our knowledge, attempts to model both *vivax* and *falciparum* ([26], [27]) at the population level do not include the possibility of co-infection. Chiyaka et al. [7] address co-infection in their *falciparum*-

malariae malaria model, however the symmetric nature of this model does not lend itself well to the application to *falciparum* and *vivax*. Our *falciparum-vivax* model addresses the need for a model that considers not only the possibility of co-infection, but also the characteristics of *vivax* that differentiate it from *falciparum*.

Competition between species can have a profound effect on survival. We have shown with our model, by studying the invasion boundaries, that two species can coexist, even if the isolated reproduction number of one of the species is less than one. This has important consequences for malaria control, since reducing one of the reproduction numbers below one may not be sufficient to eradicate either pathogen or the disease.

The emergence of parasite resistance to drug therapies is also of great concern since this foreboding obstacle poses a threat to the success of malaria control. While we do not address parasite resistance directly in our model, the fitting of several models to the enhanced malaria control period suggested that sufficient use of bednets may be able to counteract the negative effects of increased resistance to the treatment of malaria. In fact, the model selected as the best model for the majority of the bootstrapped samples (54.4% of the time) in Section 3.3, was one in which both biting rate and treatment recovery rates decreased after 1996. A decrease in recovery rate increases the average time to recovery following the administration of anti-malarial drugs. As expected, our top model indicates that decreasing biting rate and increasing the time to recovery following treatment have opposing effects on the reproduction number.

Incorporating both *P. falciparum* and *P. vivax* malaria into our model provided us with a way to determine what the most likely outcomes are for malaria in India. Bootstrapping of the best post-1996 model (model \mathcal{A}) yielded that *P. vivax* outcompeting *P. falciparum* is the most likely outcome, while the probability of extinction is only slightly more probable than the probability that *falciparum* will outcompete *vivax* malaria (22.5% versus 19.2%). The remaining candidate models predicted that *P. falciparum* outcompeting *vivax* is the most likely outcome. A side-by-side comparison of the histograms of the reproduction numbers and the invasion numbers revealed that the variance in R_{Cf} was always less than the variance in R_v^f . Conversely, the variance in R_{Cv} is greater than that of R_f^v . This means that estimating the reproduction numbers alone may not be a good predictor of the outcome of the disease.

The application of our mathematical model to data suggested that the future of malaria in India is uncertain. Although we addressed the uncertainty in the model predictions, it's important for us to note that applying the same methods to data sets for smaller regions is likely to produce very different results. In the future, we hope to use the framework we have developed here to make more confident predictions about the outcome of malaria in various regions of India.

Acknowledgments

Olivia Prosper and Maia Martcheva would like to thank Dr. Christina Chiyaka for her input during the early stages in the development of the model presented here. Olivia Prosper would also like to acknowledge support from IGERT grant NSF DGE-0801544.

A Appendix

A.1 Finding R_C using the Next-Generation approach

R_C is a threshold criterion that determines whether *P. vivax* or *P. falciparum* will be able to invade the disease-free equilibrium.

Following the approach of Diekmann et al. [11], we consider a subset of our system comprising only of equations for the infected state variables. We order these equations as follows:

$\{j'_v, L', C'_v, I'_v, j'_f, C'_f, I'_f, C'_{vf}, C'_{fv}, I'_c\}$. Next, we write the Jacobian (evaluated at the disease-free equilibrium) J of the subsystem as the difference of two matrices F and V ($J = F - V$). We choose these matrices such that the elements of F include only new infections and the remaining transitions (recovery, relapse, death, or progression to a new disease state) appear in the V matrix,

giving us $F = \begin{pmatrix} F_1 & F_2 \\ F_3 & 0 \end{pmatrix}$ where,

$$F_1 = \begin{pmatrix} 0 & 0 & 0 & f_{1,4} & 0 \\ f_{2,1} & 0 & \cdots & \cdots & 0 \\ 0 & \vdots & \ddots & & \vdots \\ 0 & \vdots & & \ddots & \vdots \\ 0 & 0 & \cdots & \cdots & 0 \end{pmatrix}, F_2 = \begin{pmatrix} 0 & 0 & f_{1,8} & 0 & f_{1,10} \\ 0 & 0 & \cdots & \cdots & 0 \\ 0 & \vdots & \ddots & & \vdots \\ 0 & 0 & & 0 & 0 \\ 0 & f_{5,7} & 0 & f_{5,9} & f_{5,10} \end{pmatrix}, F_3 = \begin{pmatrix} 0 & 0 & 0 & 0 & f_{6,5} \\ 0 & 0 & \cdots & \cdots & 0 \\ 0 & \vdots & \ddots & & \vdots \\ 0 & \vdots & & \ddots & \vdots \\ 0 & 0 & \cdots & \cdots & 0 \end{pmatrix},$$

and $V = \begin{pmatrix} V_1 & V_2 \\ 0 & V_3 \end{pmatrix}$ where,

$$V_1 = \begin{pmatrix} v_{1,1} & 0 & 0 & 0 & 0 \\ 0 & v_{2,2} & 0 & -v_{2,4} & \vdots \\ 0 & -v_{3,2} & v_{3,3} & 0 & \vdots \\ 0 & -v_{4,2} & v_{4,3} & v_{4,4} & 0 \\ 0 & \cdots & \cdots & 0 & v_{5,5} \end{pmatrix}, V_2 = \begin{pmatrix} 0 & 0 & 0 & 0 & 0 \\ 0 & 0 & \cdots & \cdots & 0 \\ 0 & \vdots & \ddots & & 0 \\ 0 & \vdots & & \ddots & -v_{4,10} \\ 0 & 0 & \cdots & \cdots & 0 \end{pmatrix},$$

$$V_3 = \begin{pmatrix} v_{66} & 0 & 0 & 0 & 0 \\ -v_{7,6} & v_{7,7} & 0 & 0 & -v_{7,10} \\ 0 & 0 & v_{8,8} & 0 & 0 \\ 0 & 0 & 0 & v_{9,9} & 0 \\ 0 & 0 & -v_{10,8} & -v_{10,9} & v_{10,10} \end{pmatrix}.$$

The nonzero elements of F are $f_{1,4} = b_v/\hat{K}$, $f_{2,1} = \beta_v/\hat{K}$, $f_{1,8} = b_v/\hat{K}$, $f_{1,10} = \zeta b_v/\hat{K}$, $f_{5,7} = b_f/\hat{K}$, $f_{5,9} = b_f/\hat{K}$, $f_{5,10} = (1 - \zeta b_f/\hat{K})$, $f_{6,5} = \sigma_f \beta_f \hat{K}$.

The nonzero elements of V are $v_{1,1} = d$, $v_{2,2} = \lambda + \mu$, $v_{2,4} = \delta$, $v_{3,2} = \sigma_v \lambda$, $v_{3,3} = \nu_v + \mu$, $v_{4,2} = (1 - \sigma_v)\lambda$, $v_{4,3} = \nu_v$, $v_{4,4} = \delta + \rho_v + \mu$, $v_{5,5} = d$, $v_{4,10} = \eta_f$, $v_{6,6} = \nu_f + \mu$, $v_{7,6} = \nu_f$, $v_{7,7} = \rho_f + \mu$, $v_{7,10} = \eta_v$, $v_{8,8} = \nu_{vf} + \mu$, $v_{9,9} = \nu_{fv} + \mu$, $v_{10,8} = \nu_{vf}$, $v_{10,9} = \nu_{fv}$, $v_{10,10} = \eta_v + \eta_f + \mu$.

If F is nonnegative and V is a nonsingular M-matrix (a Z-matrix whose eigenvalues have positive real part), then $\rho(FV^{-1}) < 1$ if and only if all eigenvalues of $J = F - V$ have negative real part (*Lemma 2* in [10]). This is equivalent to saying that if F and V satisfy these properties, then the disease free equilibrium is locally asymptotically stable only when the spectral radius (or dominant eigenvalue) of FV^{-1} is less than one. Furthermore, the inverse of an M-matrix is nonnegative [10], so that FV^{-1} is also nonnegative. FV^{-1} nonnegative implies that FV^{-1} has a positive real eigenvalue with modulus greater than or equal to all other eigenvalues of FV^{-1} [4]. In other words, $\rho(FV^{-1}) > 0$. Since $\rho(FV^{-1})$ is positive, it makes sense to define R_C to be precisely $\rho(FV^{-1})$.

Thus, to derive an expression for R_C , we must first check that F and V satisfy the appropriate conditions. Clearly F is a nonnegative matrix and V is a Z-matrix, that is, a matrix with nonpositive off-diagonal elements. One can show that a Z-matrix A is an M-matrix by showing that there exists a nonnegative vector v such that Av is positive [13].

We claim that for $v = (1, \dots, 1)^T$, $V^T v$ is positive. Since V is a Z-matrix, it is clear that V^T is also a Z-matrix. Furthermore, since V and V^T have the same eigenvalues, if V^T is an M-matrix, then so is V . Showing that $V^T v > 0$ is equivalent to showing that all row sums of V^T are positive, or equivalently that all column sums of V are positive.

It is simple to show that $S_j := \sum_{i=1}^{10} v_{i,j} > 0$ for each $j \in \{1, 2, \dots, 10\}$:

$$\begin{aligned}
S_1 &= v_{1,1} > 0 \\
S_2 &= v_{2,2} - v_{3,2} - v_{4,2} \\
&= \lambda + \mu - \sigma_v - (1 - \sigma_v) = \mu > 0 \\
S_3 &= v_{3,3} - v_{4,3} \\
&= nu_v + \mu - \nu_v = \mu > 0 \\
S_4 &= -v_{2,4} + v_{4,4} \\
&= -\delta + \delta + \rho_v + \mu = \rho_v + \mu > 0 \\
S_5 &= v_{5,5} > 0 \\
S_6 &= v_{6,6} - v_{7,6} \\
&= \nu_f + \mu - \nu_f = \mu > 0 \\
S_7 &= v_{7,7} > 0 \\
S_8 &= v_{8,8} - v_{10,8} \\
&= \nu_{vf} + \mu - \nu_{vf} = \mu > 0 \\
S_9 &= v_{9,9} - v_{10,9} \\
&= \nu_{fv} + \mu - \nu_{fv} = \mu > 0 \\
S_{10} &= -v_{4,10} - v_{7,10} + v_{10,10} \\
&= -\eta_f - \eta_v + \eta_v + \eta_f + \mu = \mu > 0.
\end{aligned}$$

Thus, V is an M-matrix, and consequently, $R_C = \rho(FV^{-1})$. To determine the expression for R_C , we first compute the inverse of V using the formula $V^{-1} = \frac{1}{\det(V)} \text{Adj}(V)$, where $\text{Adj}(V)$ is the adjugate of V . $c_{i,j} := (-1)^{(i+j)} V_{i,j}$ is called the (i,j) cofactor of V . The matrix C whose elements are the cofactors of V is called the cofactor matrix of V . The adjugate of V is defined to be the transpose of the cofactor matrix of V , that is, $\text{Adj}(V) := C^T$.

We find that $C^{-1} = \frac{1}{\det(V)} \begin{pmatrix} C_1 & C_2 \\ 0 & C_3 \end{pmatrix}$, where C_i are defined as follows for $i = 1, 2, 3$:

$$C_1 = \begin{pmatrix} c_{1,1} & 0 & 0 & 0 & 0 \\ 0 & c_{2,2} & c_{3,2} & c_{4,2} & 0 \\ 0 & c_{2,3} & c_{3,3} & c_{4,3} & 0 \\ 0 & c_{2,4} & c_{3,4} & c_{4,4} & 0 \\ 0 & 0 & 0 & 0 & c_{5,5} \end{pmatrix}, \quad C_2 = \begin{pmatrix} 0 & 0 & 0 & 0 & 0 \\ 0 & 0 & c_{8,2} & c_{9,2} & c_{10,2} \\ 0 & 0 & c_{8,3} & c_{9,3} & c_{10,3} \\ 0 & 0 & c_{8,4} & c_{9,4} & c_{10,4} \\ 0 & 0 & 0 & 0 & 0 \end{pmatrix}, \quad \text{and}$$

$$C_3 = \begin{pmatrix} 0 & 0 & 0 & 0 & 0 \\ c_{6,7} & c_{7,7} & c_{8,7} & c_{9,7} & c_{10,7} \\ 0 & 0 & c_{8,8} & 0 & 0 \\ 0 & 0 & 0 & c_{9,9} & 0 \\ 0 & 0 & c_{8,10} & c_{9,10} & c_{10,10} \end{pmatrix}.$$

Thus, $FV^{-1} = \frac{1}{\det(V)} \begin{pmatrix} K_1 & 0 & K_2 \\ 0 & K_3 & K_4 \\ 0 & 0 & 0 \end{pmatrix}$, where

$$K_1 = \begin{pmatrix} 0 & f_{1,4}c_{2,4} & f_{1,4}c_{3,4} & f_{1,4}c_{4,4} \\ f_{2,1}c_{1,1} & 0 & 0 & 0 \\ 0 & 0 & 0 & 0 \\ 0 & 0 & 0 & 0 \end{pmatrix},$$

$$K_2 = \begin{pmatrix} f_{1,4}c_{8,4} + f_{1,8}c_{8,8} + f_{1,10}c_{8,10} & f_{1,4}c_{9,4} + f_{1,10}c_{9,10} & f_{1,4}c_{10,4} + f_{1,10}c_{10,10} \\ 0 & 0 & 0 \\ 0 & 0 & 0 \\ 0 & 0 & 0 \end{pmatrix}$$

$$K_3 = \begin{pmatrix} 0 & f_{5,7}c_{6,7} & f_{5,7}c_{7,7} \\ f_{6,5}c_{5,5} & 0 & 0 \\ f_{7,5}c_{5,5} & 0 & 0 \end{pmatrix}, \text{ and}$$

$$K_4 = \begin{pmatrix} f_{5,7}c_{8,7} + f_{5,10}c_{8,10} & f_{5,7}c_{9,7} + f_{5,9}c_{9,9} + f_{5,10}c_{9,10} & f_{5,7}c_{10,7} + f_{5,10}c_{10,10} \\ 0 & 0 & 0 \\ 0 & 0 & 0 \end{pmatrix}.$$

The nonzero eigenvalues of FV^{-1} are precisely the eigenvalues of $\widehat{FV^{-1}}$, where

$$\widehat{FV^{-1}} = \frac{1}{\det(V)} \begin{pmatrix} \hat{K}_1 & 0 \\ 0 & \hat{K}_2 \end{pmatrix},$$

$$\text{and } \hat{K}_1 = \begin{pmatrix} 0 & f_{1,4}c_{2,4} \\ f_{2,1}c_{1,1} & 0 \end{pmatrix} \text{ and } \hat{K}_2 = \begin{pmatrix} 0 & f_{5,7}c_{6,7} & f_{5,7}c_{7,7} \\ f_{6,5}c_{5,5} & 0 & 0 \\ f_{7,5}c_{5,5} & 0 & 0 \end{pmatrix}.$$

Since $\widehat{FV^{-1}}$ is block triangular, its eigenvalues are the eigenvalues of $\hat{K}_1/\det(V)$ and $\hat{K}_2/\det(V)$.

Using the formula for the elements $c_{i,j}$ of the cofactor matrix C , we find that

$$\begin{aligned}
c_{1,1} &= [v_{2,2}v_{3,3}v_{4,4} - v_{2,4}(v_{3,2}v_{4,3} + v_{3,3}v_{4,2})](v_{5,5}v_{6,6}v_{7,7}v_{8,8}v_{9,9}v_{10,10}) \\
c_{2,4} &= v_{1,1}(v_{32}v_{43} + v_{33}v_{42})v_{5,5}v_{6,6} \cdots v_{10,10} \\
c_{5,5} &= v_{1,1}[v_{2,2}v_{3,3}v_{4,4} - v_{24}(v_{32}v_{43} + v_{33}v_{42})]v_{6,6} \cdots v_{10,10} \\
c_{6,7} &= v_{1,1}v_{5,5}v_{7,6}[v_{2,2}v_{3,3}v_{4,4} - v_{24}(v_{32}v_{43} + v_{33}v_{42})]v_{8,8} \cdots v_{10,10} \\
c_{7,7} &= v_{1,1}v_{5,5} \cdots v_{10,10}[v_{2,2}v_{3,3}v_{4,4} - v_{24}(v_{32}v_{43} + v_{33}v_{42})].
\end{aligned}$$

The determinant of V is $\det(V) = v_{1,1}v_{2,2} \cdots v_{10,10}[1 - k_{2,4}(k_{3,2}k_{4,3} + k_{4,2})]$, where $k_{i,j}$ denotes $v_{i,j}/v_{j,j}$.

By finding the roots of the characteristic polynomials of \hat{K}_1 and \hat{K}_2 , we arrive at the analytic expression for R_C : $R_C = \max\{R_{C_v}, R_{C_f}\}$, where R_{C_v} and R_{C_f} are as described in section 2.6.

A.2 Finding R_v^f using the Next-Generation approach

The procedure for finding an analytic expression for the invasion reproduction numbers R_v^f and R_f^v , although more challenging to carry-out, is identical to the procedure presented in A.1 for deriving R_C . The infected subsystem will now consist only of equations for state variables infected with *P. vivax*, since we want to determine the stability of the *falciparum*-only equilibrium when *vivax* attempts to invade. We first find the Jacobian of our infected subsystem, evaluated at the *falciparum*-only equilibrium, with the equations ordered as follows: $\{j'_v, L', C'_v, I'_v, C'_{vf}, C'_{fv}, I'_c\}$. We write $J = F - V$, where F and V are 7×7 square matrices and

$$F = \begin{pmatrix} 0 & 0 & 0 & f_{1,4} & f_{1,5} & 0 & f_{1,7} \\ f_{2,1} & 0 & \cdots & \cdots & \cdots & \cdots & 0 \\ 0 & \vdots & \ddots & & & & \vdots \\ 0 & \vdots & & \ddots & & & \vdots \\ 0 & \vdots & & & \ddots & & \vdots \\ f_{6,1} & \vdots & & & & \ddots & \vdots \\ 0 & 0 & \cdots & \cdots & \cdots & \cdots & 0 \end{pmatrix} \text{ and } V = \begin{pmatrix} v_{1,1} & 0 & \cdots & \cdots & 0 & \cdots & 0 \\ 0 & v_{2,2} & 0 & -v_{2,4} & \vdots & \ddots & \vdots \\ \vdots & -v_{3,2} & v_{3,3} & 0 & 0 & \cdots & 0 \\ \vdots & -v_{4,2} & -v_{4,3} & v_{4,4} & 0 & 0 & -v_{4,7} \\ \vdots & -v_{5,2} & 0 & -v_{5,4} & v_{5,5} & 0 & 0 \\ 0 & \cdots & \cdots & \cdots & 0 & v_{6,6} & 0 \\ 0 & \cdots & \cdots & 0 & -v_{7,5} & -v_{7,6} & v_{7,7} \end{pmatrix}.$$

where the elements of F are: $f_{1,4} = b_v(1 - j_v^*)/\hat{K}$, $f_{1,5} = f_{1,4}$, $f_{1,7} = \zeta f_{1,4}$, $f_{2,1} = \beta_v S^*$, and $f_{6,1} = \alpha_f \beta_v I_f^*$.

The elements of V are: $v_{1,1} = d$, $v_{2,2} = \alpha_v \beta_f j_f^* + \lambda + \mu$, $v_{2,4} = \delta$, $v_{3,2} = \sigma_v \lambda$, $v_{3,3} = \nu_v + \mu$, $v_{4,2} = (1 - \sigma_v)\lambda$, $v_{4,3} = \nu_v$, $v_{4,4} = \alpha_v \beta_f j_f^* + \delta + \rho_v + \mu$, $v_{4,7} = \eta_f$, $v_{5,2} = \alpha_v \beta_f j_f^*$, $v_{5,4} = v_{5,2}$, $v_{5,5} = \nu_{vf} + \mu$, $v_{7,5} = \nu_{vf}$, $v_{7,6} = \nu_{fv}$, $v_{7,7} = \eta_v + \eta_f + \mu$.

Again, it is clear that V has the Z-sign pattern. So, as described in A.1, it is straightforward to show that V is an M-matrix by verifying that all column-sums of V are positive. The inverse of V has the following form, where the dots represent zeros:

$$V^{-1} = \begin{pmatrix} \widehat{v}_{1,1} & \cdot & \cdot & \cdot & \cdot & \cdot & \cdot \\ \cdot & \widehat{v}_{2,2} & \widehat{v}_{2,3} & \widehat{v}_{2,4} & \widehat{v}_{2,5} & \widehat{v}_{2,6} & \widehat{v}_{2,7} \\ \cdot & \widehat{v}_{3,2} & \widehat{v}_{3,3} & \widehat{v}_{3,4} & \widehat{v}_{3,5} & \widehat{v}_{3,6} & \widehat{v}_{2,7} \\ \cdot & \widehat{v}_{4,2} & \widehat{v}_{4,3} & \widehat{v}_{4,4} & \widehat{v}_{4,5} & \widehat{v}_{4,6} & \widehat{v}_{4,7} \\ \cdot & \widehat{v}_{5,2} & \widehat{v}_{5,3} & \widehat{v}_{5,4} & \widehat{v}_{5,5} & \widehat{v}_{5,6} & \widehat{v}_{5,7} \\ \cdot & \cdot & \cdot & \cdot & \cdot & \widehat{v}_{6,6} & \cdot \\ \cdot & \widehat{v}_{7,2} & \widehat{v}_{7,3} & \widehat{v}_{7,4} & \widehat{v}_{7,5} & \widehat{v}_{7,6} & \widehat{v}_{7,7} \end{pmatrix}.$$

So,

$$FV^{-1} = \begin{pmatrix} \cdot & f_{1,4}\widehat{v}_{4,2} & f_{1,4}\widehat{v}_{4,3} & f_{1,4}\widehat{v}_{4,4} & f_{1,4}\widehat{v}_{4,5} & f_{1,4}\widehat{v}_{4,6} & f_{1,4}\widehat{v}_{4,7} \\ \cdot & +f_{1,5}\widehat{v}_{5,2} & +f_{1,5}\widehat{v}_{5,3} & +f_{1,5}\widehat{v}_{5,4} & +f_{1,5}\widehat{v}_{5,5} & +f_{1,5}\widehat{v}_{5,6} & +f_{1,5}\widehat{v}_{5,7} \\ +f_{1,7}\widehat{v}_{7,2} & +f_{1,7}\widehat{v}_{7,3} & +f_{1,7}\widehat{v}_{7,4} & +f_{1,7}\widehat{v}_{7,5} & +f_{1,7}\widehat{v}_{7,6} & +f_{1,7}\widehat{v}_{7,7} & \cdot \\ f_{2,1}\widehat{v}_{1,1} & \cdot & \cdot & \cdot & \cdot & \cdot & \cdot \\ \cdot & \cdot & \cdot & \cdot & \cdot & \cdot & \cdot \\ \cdot & \cdot & \cdot & \cdot & \cdot & \cdot & \cdot \\ \cdot & \cdot & \cdot & \cdot & \cdot & \cdot & \cdot \\ f_{6,1}\widehat{v}_{1,1} & \cdot & \cdot & \cdot & \cdot & \cdot & \cdot \\ \cdot & \cdot & \cdot & \cdot & \cdot & \cdot & \cdot \end{pmatrix}$$

The nonzero eigenvalues of FV^{-1} are precisely the nonzero eigenvalues of the 3x3 matrix

$$\widehat{FV^{-1}} = \begin{pmatrix} \cdot & f_{1,4}\widehat{v}_{4,2} & f_{1,4}\widehat{v}_{4,6} \\ \cdot & +f_{1,5}\widehat{v}_{5,2} & +f_{1,5}\widehat{v}_{5,6} \\ +f_{1,7}\widehat{v}_{7,2} & +f_{1,7}\widehat{v}_{7,3} & +f_{1,7}\widehat{v}_{7,6} \\ f_{2,1}\widehat{v}_{1,1} & \cdot & \cdot \\ f_{6,1}\widehat{v}_{1,1} & \cdot & \cdot \end{pmatrix}.$$

The characteristic polynomial of $\widehat{FV^{-1}}$ is given by $p(\tau) = |\widehat{FV^{-1}} - \tau I| = \tau[k_{6,1}(f_{1,4}\widehat{v}_{4,6} + f_{1,5}\widehat{v}_{5,6} + f_{1,7}\widehat{v}_{7,6}) + k_{2,1}(f_{1,4}\widehat{v}_{4,2} + f_{1,5}\widehat{v}_{5,2} + f_{1,7}\widehat{v}_{7,2}) - \tau^2]$, where $k_{i,j} := v_{i,j}/v_{j,j}$. Since V is an M-matrix, we know that the inverse of V has only nonnegative elements. Thus, $\widehat{v}_{5,6}$, $\widehat{v}_{7,6}$, $\widehat{v}_{5,2}$, and $\widehat{v}_{7,2}$ are nonnegative, and the largest positive root of $p(\tau)$ is

$$\tau^* = \sqrt{k_{6,1}(f_{1,4}\widehat{v}_{4,6} + f_{1,5}\widehat{v}_{5,6} + f_{1,7}\widehat{v}_{7,6}) + k_{2,1}(f_{1,4}\widehat{v}_{4,2} + f_{1,5}\widehat{v}_{5,2} + f_{1,7}\widehat{v}_{7,2})}.$$

Recall that $\widehat{v}_{i,j}$ are the elements of V^{-1} . Thus, $\widehat{v}_{i,j} = (-1)^{i+j} c_{j,i}/\det(V)$, where $C := (c_{i,j})$ is the cofactor matrix of V . To determine $\widehat{v}_{4,6}$, $\widehat{v}_{5,6}$, $\widehat{v}_{7,6}$, $\widehat{v}_{4,2}$, $\widehat{v}_{5,2}$, and $\widehat{v}_{7,2}$, we need only calculate

$c_{6,4}$, $c_{6,5}$, $c_{6,7}$, $c_{2,4}$, $c_{2,5}$, $c_{2,7}$, and $\det(V)$.

$$\begin{aligned}
c_{6,4} &= v_{1,1}v_{2,2}v_{3,3}v_{5,5}v_{4,7}v_{7,6} \\
c_{6,5} &= v_{1,1}v_{7,6}v_{4,7}v_{3,3}(v_{2,2}v_{5,4} + v_{2,4}v_{5,2}) \\
c_{6,7} &= v_{1,1}v_{7,6}v_{5,5}[v_{2,2}v_{3,3}v_{4,4} - v_{2,4}(v_{3,2}v_{4,3} + v_{3,3}v_{4,2})] \\
c_{2,4} &= v_{1,1}v_{6,6}[v_{7,5}v_{5,2}v_{3,3}v_{4,7} + v_{7,7}v_{5,5}(v_{3,2}v_{4,3} + v_{3,3}v_{4,2})] \\
c_{2,5} &= v_{1,1}v_{6,6}v_{7,7}[v_{3,2}v_{4,3}v_{5,4} + v_{3,3}(v_{4,2}v_{5,4} + v_{4,4}v_{5,2})] \\
c_{2,7} &= v_{1,1}v_{6,6}v_{7,5}[v_{3,2}v_{4,3}v_{5,4} + v_{3,3}(v_{4,2}v_{5,4} + v_{4,4}v_{5,2})],
\end{aligned}$$

and

$$\begin{aligned}
\det(V) &= v_{1,1}v_{2,2} \cdots v_{7,7}[1 - k_{2,4}(k_{3,2}k_{4,3} + k_{4,2}) - k_{7,5}k_{4,7}(k_{5,4} + k_{2,4}k_{5,2})] \\
&= 1 - \frac{\delta}{\alpha_v\beta_f j_f^* + \delta + \rho_v + \mu} \left(\frac{\sigma_v \lambda}{\alpha_v\beta_f j_f^* + \lambda + \mu} \cdot \frac{\nu_v}{\nu_v + \mu} + \frac{(1 - \sigma_v)\lambda}{\alpha_v\beta_f j_f^* + \lambda + \mu} \right) \\
&\quad - \frac{\nu_{vf}}{\nu_{vf} + \mu} \cdot \frac{\eta_f}{\eta_v + \eta_f + \mu} \left(\frac{\alpha_v\beta_f j_f^*}{\alpha_v\beta_f j_f^* + \delta + \rho_v + \mu} + \frac{\delta}{\alpha_v\beta_f j_f^* + \delta + \rho_v + \mu} \cdot \frac{\alpha_v\beta_f j_f^*}{\alpha_v\beta_f j_f^* + \lambda + \mu} \right)
\end{aligned}$$

The invasion reproduction number $R_v^f := \tau^*$. Making the appropriate substitutions into τ^* , we arrive at the expression for R_v^f in section 2.8

A.3 Finding R_f^v using the Next-Generation approach

To derive R_f^v , we find the Jacobian of the *falciparum*-infected subsystem, with the order: $\{j'_f, C'_f, I'_f, C'_{vf}, C'_{fv}, I'_c\}$. The Jacobian evaluated at the *vivax*-only equilibrium is given by $J = F - V$, where

$$F = \begin{pmatrix} 0 & 0 & f_{1,3} & 0 & f_{1,5} & f_{1,6} \\ f_{2,1} & 0 & \cdots & \cdots & \cdots & 0 \\ f_{3,1} & \vdots & \ddots & & & \vdots \\ f_{4,1} & \vdots & & \ddots & & \vdots \\ 0 & \vdots & & & \ddots & \vdots \\ 0 & 0 & 0 & 0 & 0 & 0 \end{pmatrix}, \text{ and } V = \begin{pmatrix} v_{1,1} & 0 & 0 & 0 & 0 & 0 \\ 0 & v_{2,2} & 0 & 0 & 0 & 0 \\ 0 & -v_{3,2} & v_{3,3} & 0 & 0 & -v_{3,6} \\ 0 & 0 & 0 & v_{4,4} & 0 & 0 \\ 0 & 0 & -v_{5,3} & 0 & v_{5,5} & 0 \\ 0 & 0 & 0 & -v_{6,4} & -v_{6,5} & v_{6,6} \end{pmatrix},$$

where $f_{1,3} = b_f(1 - j_v^*)\hat{K}$, $f_{1,5} = f_{1,3}$, $f_{1,6} = (1 - \zeta)f_{1,3}$, $f_{2,1} = \sigma_f\beta_f S^*$, $f_{3,1} = (1 - \sigma_f)S^*$, $f_{4,1} = \alpha_v\beta_f(I_v^* + L^*)$, and $v_{1,1} = d$, $v_{2,2} = \nu_f + \mu$, $v_{3,2} = \nu_f$, $v_{3,6} = \eta_v$, $v_{4,4} = \nu_{vf} + \mu$, $v_{5,3} = \alpha_f\beta_v j_v^*$, $v_{5,5} = \nu_{fv} + \mu$, $v_{6,4} = \nu_{vf}$, $v_{6,5} = \nu_{fv}$, $v_{6,6} = \eta_v + \eta_f + \mu$.

F is nonnegative and V is a nonsingular Z-matrix. We show, as we did in appendices A.1 and A.2, that V is also an M-matrix by showing that the column sums of V are positive. Since each

$v_{i,j} > 0$ and $v_{2,2} > v_{3,2}$, $v_{3,3} > v_{5,3}$, $v_{4,4} > v_{6,4}$, $v_{5,5} > v_{6,5}$, and $v_{6,6} > v_{3,6}$, each column sum is positive, and hence V is a nonsingular M-matrix. Thus, V^{-1} is nonnegative (hence FV^{-1} is also nonnegative) and all eigenvalues of J have negative real part if and only if $R_f^v := \rho(FV^{-1}) < 1$. Using the notation that $C := (c_{i,j})$ is the cofactor matrix of V , we have that

$$V^{-1} = \frac{1}{\det(V)} \cdot \begin{pmatrix} c_{1,1} & \cdot & \cdot & \cdot & \cdot & \cdot \\ \cdot & c_{2,2} & \cdot & \cdot & \cdot & \cdot \\ \cdot & c_{2,3} & c_{3,3} & c_{4,3} & c_{5,3} & c_{6,3} \\ \cdot & \cdot & \cdot & c_{4,4} & \cdot & \cdot \\ \cdot & c_{2,5} & c_{3,5} & c_{4,5} & c_{5,5} & c_{6,5} \\ \cdot & c_{2,6} & c_{3,6} & c_{4,6} & c_{5,6} & c_{6,6} \end{pmatrix}.$$

So,

$$FV^{-1} = \frac{1}{\det(V)} \cdot \begin{pmatrix} 0 & f_{1,3}c_{2,3} & f_{1,3}c_{3,3} & f_{1,3}c_{4,3} & f_{1,3}c_{5,3} & f_{1,3}c_{6,3} \\ 0 & +f_{1,5}c_{2,5} & +f_{1,5}c_{3,5} & +f_{1,5}c_{4,5} & +f_{1,5}c_{5,5} & +f_{1,5}c_{6,5} \\ f_{2,1}c_{1,1} & +f_{1,6}c_{2,6} & +f_{1,6}c_{3,6} & +f_{1,6}c_{4,6} & +f_{1,6}c_{5,6} & +f_{1,6}c_{6,6} \\ f_{2,1}c_{1,1} & 0 & \cdots & \cdots & \cdots & 0 \\ f_{3,1}c_{1,1} & \vdots & \ddots & & & \vdots \\ f_{4,1}c_{1,1} & \vdots & & \ddots & & \vdots \\ 0 & \vdots & & & \ddots & \vdots \\ 0 & 0 & 0 & 0 & 0 & 0 \end{pmatrix}$$

Observe that the nonzero eigenvalues of FV^{-1} are exactly the nonzero eigenvalues of

$$\widehat{FV^{-1}} = \frac{1}{\det(V)} \cdot \begin{pmatrix} 0 & f_{1,3}c_{2,3} & f_{1,3}c_{3,3} & f_{1,3}c_{4,3} \\ 0 & +f_{1,5}c_{2,5} & +f_{1,5}c_{3,5} & +f_{1,5}c_{4,5} \\ f_{2,1}c_{1,1} & +f_{1,6}c_{2,6} & +f_{1,6}c_{3,6} & +f_{1,6}c_{4,6} \\ f_{2,1}c_{1,1} & 0 & \cdots & 0 \\ f_{3,1}c_{1,1} & \vdots & \ddots & \vdots \\ f_{4,1}c_{1,1} & 0 & \cdots & 0 \end{pmatrix}, \text{ where}$$

$$\begin{aligned}
c_{1,1} &= v_{2,2} \cdots v_{6,6} (1 - k_{3,6} k_{5,3} k_{6,5}) \\
c_{2,3} &= v_{1,1} v_{4,4} v_{5,5} v_{6,6} v_{3,2} \\
c_{3,3} &= v_{1,1} v_{2,2} v_{4,4} v_{5,5} v_{6,6} \\
c_{4,3} &= v_{1,1} v_{2,2} v_{5,5} v_{3,6} v_{6,4} \\
c_{2,5} &= v_{1,1} v_{4,4} v_{6,6} v_{3,2} v_{5,3} \\
c_{3,5} &= v_{1,1} v_{2,2} v_{4,4} v_{6,6} v_{5,3} \\
c_{4,5} &= v_{1,1} v_{2,2} v_{5,3} v_{3,6} v_{6,4} \\
c_{2,6} &= v_{1,1} v_{4,4} v_{3,2} v_{5,3} v_{6,5} \\
c_{3,6} &= v_{1,1} v_{2,2} v_{4,4} v_{5,3} v_{6,5} \\
c_{4,6} &= v_{1,1} v_{2,2} v_{3,3} v_{5,5} v_{6,4}, \quad \text{and}
\end{aligned}$$

$$\det(V) = v_{1,1} \cdots v_{6,6} (1 - k_{3,6} k_{5,3} k_{6,5}).$$

Recall (from the previous appendices) that $k_{i,j} := v_{i,j}/v_{j,j}$.

The only positive root of the characteristic polynomial $p(\tau) = |\widehat{FV}^{-1} - \tau I|$ is $\tau^* = \sqrt{a_1 + a_2 + a_3}$, where

$$\begin{aligned}
a_1 &= \frac{k_{2,1}}{1 - k_{3,6} k_{5,3} k_{6,5}} \cdot (k_{3,2} k_{1,3} + k_{3,2} k_{5,3} k_{1,5} + k_{3,2} k_{5,3} k_{6,5} k_{1,6}) \\
a_2 &= \frac{k_{3,1}}{1 - k_{3,6} k_{5,3} k_{6,5}} (k_{1,3} + k_{5,3} k_{1,5} + k_{5,3} k_{6,5} k_{1,6}) \\
a_3 &= \frac{k_{4,1}}{1 - k_{3,6} k_{5,3} k_{6,5}} \cdot (k_{6,4} k_{1,6} + k_{6,4} k_{3,6} k_{1,3} + k_{6,4} k_{3,6} k_{5,3} k_{1,5}).
\end{aligned}$$

Since the invasion number R_f^v is defined to be the dominant eigenvalue of FV^{-1} , $R_f^v = \tau^* = \sqrt{a_1 + a_2 + a_3}$, the expression presented in section 2.8.

References

- [1] T. ADAK, V. P. SHARMA, AND V. S. ORLOV, *Studies on the Plasmodium vivax relapse pattern in Delhi, India*, Am. J. Trop. Med. Hyg., 59 (1998), pp. 175–179.
- [2] N. T. J. BAILEY, *The Biomathematics of Malaria*, Charles Griffin & Company LTD, London, 1982.
- [3] T. BARIK, B. SAHU, AND V. SWAIN, *A review on Anopheles culicifacies: From bionomics to control with special reference to Indian subcontinent*, Acta Tropica, 109 (2009), pp. 87 – 97.

- [4] A. BERMAN AND R. J. PLEMMONS, *Nonnegative Matrices in the Mathematical Sciences*, Academic, New York, 1970.
- [5] K. P. BURNHAM AND D. R. ANDERSON, *Multimodel inference: Understanding AIC and BIC in model selection*, *Sociological Methods Research*, 33 (2004), pp. 193–204.
- [6] *Malaria facts*, CDC.
- [7] C. CHIYAKA, Z. MUKANDAVIRE, P. DAS, F. NYABADZA, S. D. HOVE-MUSEKWA, AND H. MWAMBI, *Theoretical analysis of mixed plasmodium malariae and plasmodium falciparum infections with partial cross-immunity*, *Journal of Theoretical Biology*, 263 (2010), pp. 169 – 178.
- [8] G. CHOWELL, C. AMMON, N. HENGARTNERA, AND J. HYMAN, *Transmission dynamics of the great influenza pandemic of 1918 in geneva, switzerland: Assessing the effects of hypothetical interventions*, *Journal of Theoretical Biology*, 241 (2006), pp. 193–204.
- [9] National Vector Borne Disease Control Programme.
- [10] O. DIEKMANN AND J. A. P. HEESTERBEEK, *Mathematical epidemiology*, Springer, 2008, ch. Further notes on the basic reproduction number.
- [11] O. DIEKMANN, J. A. P. HEESTERBEEK, AND M. G. ROBERTS, *The construction of next-generation matrices for compartmental epidemic models*, *J. R. Soc. Intergace*, (2009).
- [12] C. J. FEIGIN RD, *Textbook of Pediatric Infectious Diseases. 5th ed. Vol 2.*, Saunders, Philadelphia, PA, 2004.
- [13] M. FIEDLER, *Special Matrices and Their Applications in Numerical Mathematics*, Martinus Nijhoff, Dordrecht, 1986.
- [14] B. GUPTA, P. GUPTA, A. SHARMA, V. SINGH, A. P. DASH, AND A. DAS, *High proportion of mixed-species plasmodium infections in india revealed by pcr diagnostic assay*, *Tropical Medicine & International Health*, 15 (July 2010).
- [15] D. HAMER, M. SINGH, B. WYLIE, K. YEBOAH-ANTWI, J. TUCHMAN, M. DESAI, V. UD-HAYAKUMAR, P. GUPTA, M. BROOKS, M. SHUKLA, K. AWASTHY, L. SABIN, W. MACLEOD, A. DASH, AND N. SINGH, *Burden of malaria in pregnancy in jharkhand state, india*, *Malaria Journal*, 8 (2009), p. 210.
- [16] H. JOSHI, S. K. PRAJAPATI, A. VERMA, S. KANG'A, AND J. M. CARLTON, *Plasmodium vivax in india*, *Trends in Parasitology*, 24 (2008), pp. 228 – 235.
- [17] A. KUMAR, N. VALECHA, T. JAIN, AND A. P. DASH, *Burden of malaria in India: Retrospective and prospective view*, *Am. J. Trop. Med. Hyg.*, 77 (2007), pp. 69 – 78.
- [18] S. LAWPOOLSRI, E. KLEIN, P. SINGHASIVANON, S. YIMSAMRAN, N. THANYAVANICH, W. MANEEBOONYANG, L. HUNGERFORD, J. MAGUIRE, AND D. SMITH, *Optimally tim-*

- ing primaquine treatment to reduce plasmodium falciparum transmission in low endemicity thai-myanmar border populations*, *Malaria Journal*, 8 (2009), p. 159.
- [19] *Life expectancy at birth, total (years)*, The World Bank.
- [20] M. MAYXAY, S. PUKRITRAYAKAMEE, K. CHOTIVANICH, M. IMWONG, S. LOOAREESUWAN, AND N. WHITE, *Identification of cryptic coinfection with plasmodium falciparum in patients presenting with vivax malaria*, *Am J Trop Med Hyg*, 65 (2001), pp. 588–592.
- [21] M. MAYXAY, S. PUKRITTAYAKAMEE, P. N. NEWTON, AND N. J. WHITE, *Mixed-species malaria infections in humans*, *Trends in Parasitology*, 20 (2004), pp. 233 – 240.
- [22] M. NACHER, U. SILACHAMROON, P. SINGHASIVANON, P. WILAIRATANA, W. PHUMRATANAPRAPIN, A. FONTANET, AND S. LOOAREESUWAN, *Comparison of artesunate and chloroquine activities against plasmodium vivax gametocytes*, *Antimicrob. Agents Chemother.*, 48 (2004), pp. 2751–2752.
- [23] *Guidelines for diagnosis and treatment of malaria in india - 2009*, National Vector Borne Disease Control Programme.
- [24] G. T. PHAN, P. J. DE VRIES, B. Q. TRAN, H. Q. LE, N. V. NGUYEN, T. V. NGUYEN, S. H. HEISTERKAMP, AND P. A. KAGER, *Artemisinin or chloroquine for blood stage plasmodium vivax malaria in vietnam*, *Tropical Medicine & International Health*, 7 (2002), pp. 858–864.
- [25] W. PHIMPRAPHI, R. PAUL, S. YIMSAMRAN, S. PUANGSA-ART, N. THANYAVANICH, W. MANEEBOONYANG, S. PROMMONGKOL, S. SORNKLOM, W. CHAIMUNGKUN, I. CHAVEZ, H. BLANC, S. LOOAREESUWAN, A. SAKUNTABHAI, AND P. SINGHASIVANON, *Longitudinal study of plasmodium falciparum and plasmodium vivax in a karen population in thailand*, *Malar J*, 7 (2008), p. 99.
- [26] P. PONGSUMPUN AND I.M.TANG, *The transmission model of P.falciparum and P.vivax malaria between Thai and Burmese*, *International Journal of Mathematical Models and Methods in Applied Sciences*, 3 (2004), pp. 19–26.
- [27] ———, *Impact of cross-border migration on disease epidemics: case of the P. falciparum and P. vivax malaria epidemic along the thai-myanmar border*, *Journal of Biological Systems*, 18 (2010), pp. 55–73.
- [28] *International data base (IDB)*, U.S. Census Bureau.
- [29] R. N. PRICE, E. TJITRA, C. A. GUERRA, S. YEUNG, N. J. WHITE, AND N. M. ANSTEY, *Vivax malaria: neglected and not benign*, *Am. J. Trop. Med. Hyg.*, 77(Suppl 6) (2007), pp. 79–87.
- [30] G. SNOUNOU AND N. J. WHITE, *The co-existence of plasmodium: sidelights from falciparum and vivax malaria in thailand*, *Trends in Parasitology*, 20 (2004), pp. 333 – 339.

- [31] P. VAN DEN DRIESSCHE AND J. WATMOUGH, *Reproduction numbers and sub-threshold endemic equilibria for compartmental models of disease transmission*, *Mathematical Biosciences*, 180 (2002), pp. 29–48.
- [32] *10 facts on malaria*, WHO.
- [33] P. WILAIRATANA, N. TANGPUKDEE, S. KANO, AND S. KRUDSOOD, *Primaquine administration after falciparum malaria treatment in malaria hypoendemic areas with high incidence of falciparum and vivax mixed infection: Pros and cons*, *The Korean Journal of Parasitology*, 48 (2010), pp. 175 – 177.